Hydraulics Research
Wallingford

LOCAL SCOUR AROUND LARGE OBSTRUCTIONS

By

R W P May and I R Willoughby

Report SR240
March 1990

Registered Office: Hydraulics Research Limited,
Wallingford, Oxfordshire OX10 8BA.
Telephone: 0491 35381. Telex: 848552

This report describes work funded by the Department of the Environment under Research Contract No PECD 7/6/113, Hydraulic Structures and Alluvial Processes. It is published on behalf of the Department of the Environment, but any opinions expressed in this report are not necessarily those of the funding Department. The work was carried out in the River Engineering Department of Hydraulics Research, Wallingford headed by Dr W R White. The nominated project officers were Dr R P Thorogood and Mr P Woodhead for DOE and Dr W R White for HR.

ABSTRACT

An experimental study, funded by the Department of the Environment, was made to determine the depth of local scour around large obstructions such as caissons and cofferdams used during the construction of bridges across rivers and estuaries. These structures are usually larger than the completed bridge piers so the construction phase can be more critical in terms of scour depth. Model and prototype data for large obstructions are limited but suggest that existing design formulae tend to overestimate the amount of scour. The present study therefore concentrated on cases where the width of the structure was large in relation to the depth of flow.

The experiments were carried out in a 2.4m wide flume using square and circular vertical piers with widths of B = 0.1m, 0.2m and 0.4m; the square piers were set normal to the flow. A uniform sand with a mean size of d_{50}= 0.145mm was used as the mobile bed material. The main scour tests were carried out using a mean flow velocity U below the threshold value U_c for general bed movement. This was done in order to limit scour to the available depth in the flume and to prevent the formation of a rippled bed. Tests were made at flow depths of y_o= 0.05m, 0.10m, 0.20m and 0.40m, giving ratios of depth to pier size in the range y_o/B = 0.125 to 4.0. Each test was continued until the scour depth was considered to be at or close to equilibrium, and durations varied from 44 hours to about 72 hours. A detailed survey of the scour hole was made at the end of each test.

A second set of tests was carried out with one square and one circular pier to determine the relationships between scour depth and flow velocity. In the case of the square pier, scour was found to start at a velocity of about U = 0.375 U_c and to increase linearly with increasing velocity up to U = U_c In the case of the circular pier, scour started at about U = 0.5 U_c and varied non-linearly with velocity.

These depth/velocity relationships were then used in the analysis of the results from the main scour tests. For given flow conditions, the depth of scour at a square pier (at zero angle of incidence) was on average 1.33 times the depth at a circular pier of equal width. The results for both pier types were combined to produce a single relationship describing the effect of relative flow depth y_o/B on the depth of scour. As expected, this was found to predict significantly less scour than two existing design formulae when the relative flow depth y_o/B was < 1.

The results of the study were summarised in a set of equations which take account of pier size and shape, flow depth and flow velocity. The equations give estimates of scour in uniform sediments that are conservative relative to all the tests carried out in the present study. The new equations are considered to be more accurate (and economical) than existing design formulae when applied to large obstructions such as cofferdams in relatively shallow water.

SYMBOLS

a	Constant in Equation (5)
B	Width of pier normal to longitudinal centreline
c	Constant in Equation (23)
D	Duration of test
d	Sediment size
d_{max}	Maximum particle size in grading
d_n	Size not exceeded by n% of sediment by weight
d_{50}	Mean particle size
d_{50a}	Mean particule size of armoured bed
F_d	Function describing effect of sediment size, Equation (20)
F_s	Function describing effect of pier shape
F_u	Function describing effect of flow velocity, Equation (18)
F_y	Function describing effect of flow depth, Equation (19)
f_s	Function describing effect of pier shape, Equation (9)
f_u	Function describing effect of flow velocity, Equation (8)
f_α	Function describing effect of angle of incidence
g	Acceleration due to gravity
L	Length of pier parallel to longitudinal centreline
R_*	Particle Reynolds number
s	Relative specific gravity of sediment
t	Time
U	Depth-averaged flow velocity
U'	Notional velocity, Equation (17)

SYMBOLS (Cont'd)

U_a	Maximum value of U resisted by armoured bed
U_c	Value of U at threshold of sediment movement
U_{ca}	Maximum possible value of U_c for armoured bed
u_*	Shear velocity
u_{*c}	Shear velocity at threshold of sediment movement
y_o	Depth of flow
y_s	Equilibrium depth of scour below bed level
y_{sc}	Value of y_s at threshold condition ($U/U_c = 1$)
y_{sl}	Scour depth on left-hand side of pier
y_{sm}	Maximum value of y_{sc} in deep water
y_t	Depth of scour at time t
α	Angle of incidence between flow and pier centreline
β	Factor in Equation (4)
γ	Coefficient in Equation (23)
ν	Kinematic viscosity of water
ρ	Density of water
σ_g	Geometric standard deviation of sediment grading, Equation (15)
τ	Shear stress applied by flow
τ_c	Value of τ at threshold of sediment movement
Ψ_s	Shields parameter, Equation (1)

CONTENTS

TABLES

FIGURES

FIGURES (CONT)

1 INTRODUCTION

A structure located in flowing water produces a complex three-dimensional flow pattern that may cause localised scouring of a sand or gravel bed. The foundations of bridges which cross alluvial channels can therefore be undermined by local scour, and failures have occurred fairly regularly in the UK and around the world. As a result, much experimental research has been carried out on local scour in order to identify the mechanisms involved and develop methods of prediction. The subject has proved to be very complex, but it is now possible to estimate scour depths with reasonable accuracy for simple shapes of pier that are relatively slender in relation to the depth of flow (see for example Melville & Sutherland (1988)).

It has been found from many small-scale studies that maximum depths of scour are typically between 1.5 times and 3.0 times the width of the structure, and these results are supported reasonably well by field measurements of scour at bridge piers. However, as pointed out by Carstens & Sharma (1975), simple geometric scaling seems unreasonable when applied to large marine structures such as oil production platforms which can have diameters of the order of 100m. It is likely in such cases that other factors associated with the structure of turbulent flows intervene to prevent the occurrence of very large scour depths.

A similar but less extreme scale problem occurs with cofferdams and caissons used during the construction of river and estuary crossings. These structures are usually much larger than the final bridge piers, and can therefore represent a more critical design condition. Limited research has indicated that scour depths are reduced when a structure is large in relation to the depth of flow. However, results from some model studies of bridge crossings carried out by Hydraulics Research indicated that existing formulae tended to overestimate scour depths at large obstructions such as cofferdams. The present study was therefore designed to investigate systematically the effect of structure size in relatively shallow flows using a large flume available at Hydraulics Research. The project was funded by the Construction Industry Directorate of the Department of the Environment as part of its research programme on hydraulic structures and alluvial processes.

2 PREVIOUS STUDIES

2.1 Mechanisms of local scour

When an obstacle is placed in flowing water it can produce general scour and local scour. General scour occurs across the whole width of a channel, and is caused by an increase in mean flow velocity resulting from the blockage due to the obstacle. By contrast, local scour is concentrated around the obstacle, and is caused by localised increases in flow velocity due to streamline curvature, turbulence and the establishment of complex vortex motions.

Local scour develops first on the sides of an obstacle where streamline curvature produces the highest mean velocities ; in the case of a vertical circular cylinder, potential flow theory predicts that the maximum velocity on the sides is equal to twice the upstream velocity. Stagnation pressures also develop on the upstream face of the obstacle, and due to the variation in velocity with depth these pressures are higher at the surface than at the bed. As a result, flow develops down the face of the obstacle and produces a notched scour hole around its upstream edge. As the scour continues at the sides, the holes extend forwards until they meet and form a single large hole upstream of the obstacle. Flow passing over this hole separates and produces a vortex rotating about a horizontal axis transverse to the flow. This is commonly termed a "horseshoe" vortex because it is U-shaped in plan with two arms which wrap around the base of the obstacle before being carried downstream by the flow. The horseshoe vortex is effective at picking up and transporting material eroded from the notch at the base of the obstacle, and is usually the dominant mechanism of local scour. The principal features are shown diagrammatically in Figure 1.

Two other mechanisms can also cause local scour. Flow separation at the downstream end of an obstacle produces "wake" vortices which are shed periodically from either side and which rotate about a vertical axis. Reduced pressures in the vortex cores can lift sediment from the bed and transport it downstream. Wake vortices tend to produce long, relatively narrow scour holes extending downstream of the obstacle on either side.

The other mechanism is caused by flow separation at vertical changes in the cross-sectional shape of the obstacle. "Trailing" vortices are formed which normally rotate about horizontal axes parallel to the flow. Such vortices may not produce significant scour unless they are close to the bed.

Upstream of an obstacle, a re-circulating vortex forms at the water surface, as indicated in Figure 1. This vortex does not influence flow conditions at the bed when the water is deep in relation to the size of the obstacle. However, in shallow flows, the surface vortex acts to reduce the strength of the horseshoe vortex which is of opposite sign. As a result, depths of local scour tend to reduce as the flow depth decreases below a certain limit.

The horizontal extent of a scour hole depends principally on the depth of scour that develops and the angle of repose of the sediment. The plan shape of the hole is also affected by the geometry of the obstacle, and by the relative importance of the three types of vortex motion (horseshoe, wake and trailing) which give rise to the scour.

2.2 Threshold of movement

Movement of bed material occurs when the shear stress τ applied by the flow to particles at the surface exceeds a critical value τ_c. The threshold condition for non-cohesive sediment is described by the well-known Shields curve (see Henderson (1966), p.411) which defines a relationship between the Shields parameter

$$\Psi_s = \frac{\tau}{\rho g \ (s-1) \ d} \qquad (1)$$

and the particle Reynolds number

$$R_* = \frac{u_* d}{\nu} \qquad (2)$$

where u_* is the shear velocity given by

$$u_* = (\tau/\rho)^{1/2} \qquad (3)$$

and d is the particle size ; other quantities are defined in the list of Symbols at the beginning of this report. For fully-developed turbulent flow, the shear velocity is related to the flow depth y_o and the depth-averaged velocity U by the Karman-Prandtl equation

$$\frac{U}{u_*} = 5.75 \log_{10} \left(\frac{y_o}{\beta\, d_n} \right) + 6 \qquad (4)$$

where β is a constant and d_n is the particle size <u>not</u> exceeded by n% of the sediment by weight. Various researchers have used different values of β and n; Melville & Sutherland (1988) recommended β = 2 in conjunction with the mean sediment size, d_{50}. At the threshold of movement the parameters τ, u_* and U attain their critical values τ_c, u_{*c} and U_c.

Alternative formulae for determining the critical flow velocity which do not require use of the Shields curve are given by Hanco (1971)

$$U_c = a\, [g\, (s-1)\, d]^{½}\, (y_o/d)^{0.2} \qquad (5)$$

where a = 1.0 for d_{90} > 0.7mm and a = 1.2 to 1.4 for d_{90} < 0.7mm, and by Ackers & White (1973)

$$U_c = [\log_{10} (10 y_o/d_{35})\,].\, [32g\, (s-1) d_{35}]^{½}$$

$$.\ [\, 0.23\, \{ g\, (s-1)\, d_{35}^3/\nu^2\}^{-1/6} + 0.14\,] \qquad (6)$$

2.3 Experimental studies

Breusers et al (1977) made a comprehensive survey of the many studies which had previously been carried out on local scour. The principal findings can be illustrated by considering the following equation which Breusers et al recommended for predicting the equilibrium scour depth y_s at an obstruction.

$$\frac{y_s}{B} = 1.5\ f_u(U/U_c)\ .\ \tanh\ (y_o/B)\ .\ f_s(\text{shape})$$

$$.\ f_\alpha\ (\alpha,\ L/B) \qquad (7)$$

where B is the width of the structure normal to its longitudinal centreline.

The function f_u takes account of the effect of flow velocity and has the form

$$f_u = 0, \text{ for } U/U_c < 0.5 \qquad (8a)$$

$$f_u = \left(\frac{2U}{U_c} - 1\right), \text{ for } 0.5 \le U/U_c \le 1.0 \qquad (8b)$$

$$f_u = 1, \text{ for } U/U_c > 1.0 \qquad (8c)$$

This expresses the finding that local scour at an obstruction begins when the average flow velocity upstream is about 0.5 of the critical value at which the bed would begin to move in the absence of the obstruction. The scour depth then increases approximately linearly with increasing velocity until a maximum is reached when the bed is on the point of general movement (ie. $U = U_c$). "Clear-water" scour is said to occur when $U/U_c \le 1$ because there is no transport of sediment into the scour hole from upstream. When the general threshold of movement is exceeded, "live-bed" scour occurs and the scour depth fluctuates due to the periodic passage of dunes past the obstruction. The average value of the maximum scour depth under live-bed conditions is typically about 90% of the depth at the critical condition $U/U_c = 1.0$, so the maximum clear-water value represents the most severe design case. For live-bed scour, a margin of safety is necessary because of the temporal fluctuations in scour depth, so a figure of $f_u = 1$ is used for all $U/U_c \geq 1$ in Equation (8c). The multiplying factor of 1.5 represents an average value determined from a large number of studies, but Breusers et al (1977) recommended that a value of 2 should be substituted when using Equation (7) for design.

The function tanh (y_o/B) in Equation (7) takes account of the effect which the depth of flow has on local scour. When the water depth is more than two or three times the width of the obstruction, the function has effectively a constant value of 1.0. Below this approximate limit, a reduction in water depth decreases the depth of scour, as explained in Section 2.1; for very shallow flows the function is approximately equal to y_o/B.

The shape function f_s has the following recommended values:

circular and rounded piers : $f_s = 1.0$ (9a)

streamlined shapes : $f_s = 0.75$ (9b)

square and rectangular piers: $f_s = 1.3$ (9c)

The function f_α describes the effect of the angle of incidence α between the flow and the centreline of the pier. The value of f_α also depends on the length/width ratio L/B of the pier, and can be determined from curves produced by Laursen & Toch (1953). The function has a minimum value of $f_\alpha = 1.0$ when the flow is in line with the pier ($\alpha = 0$).

Breusers et al (1977) also detailed other formulae developed by earlier researchers for predicting the equilibrium scour depth, and those which are relevant to the present study include the following.

(1) Hanco (1971) - modified by Breusers et al:

$$\frac{y_s}{B} = 3.3 \left(\frac{d}{B} \right)^{0.2} \left(\frac{y_o}{B} \right)^{0.13} \qquad (10)$$

(2) Shen et al (1966) :

$$\frac{y_s}{B} = 2 \left(\frac{U^2}{g y_o} \right)^{0.215} \left(\frac{y_o}{B} \right)^{0.355} \qquad (11)$$

(3) Torsethaugen (1975) :

$$\frac{y_s}{B} = 0.9 \left(\frac{2U}{U_c} - 1.08 \right) \left(\frac{y_o}{B} \right) \qquad (12)$$

All three formulae apply to circular cylinders. Equation (12) is of particular interest because it was obtained from tests with relatively shallow flows in the range $0.2 \le y_o/B \le 0.65$; most of the experiments were carried out with $U/U_c = 0.8$.

Since 1977 significant new research has been carried out at the University of Auckland, particularly on the effects of non-uniform sediment gradings. The following is a brief summary of results reported by

Raudkivi & Ettema (1983), Melville (1984), Raudkivi (1986), Melville & Sutherland (1988) and Chiew & Melville (1989).

Equation (7) was developed mainly from data for uniformly graded sediments, and curve A in Figure 2 indicates how the scour depth varies with flow velocity for such sediments. Beyond the critical flow velocity U_c , the scour depth decreases and reaches a minimum when the dunes approaching the scour hole attain their maximum steepness. The scour depth then increases again as the dunes become flatter and reaches a second maximum when the transitional flat-bed stage occurs.

If the size of a uniform sediment is less than about 0.5mm to 0.7mm, ripples begin to form on the bed before the critical flow velocity is reached. Movement of the ripples produces a small rate of sediment transport so that clear-water scour cannot be maintained up to $U/U_c = 1.0$. As a result, the depth of scour is only about 70% of that which occurs with a coarser non-rippling sediment. At higher flow velocities, general bed movement eliminates the effect of rippling and the curves for fine and coarse sediments merge, as illustrated by curve B in Figure 2.

Scour depths are also reduced if the grading of the sediment is non-uniform, as shown by curve C in Figure 2. As the flow velocity is increased, the finer particles of the mixture are removed and the upstream bed becomes armoured with the coarser particles. As a result, clear-water scour can persist to a flow velocity which is higher than the critical velocity U_c corresponding to the mean sediment size, d_{50}, of the original mixture. The mean size, d_{50a}, of the armoured bed is related to the maximum sediment size, d_{max}, in the original mixture by

$$d_{50a} = d_{max}/1.8 \tag{13}$$

The maximum flow velocity, U_a, which the armoured bed can resist is given by

$$U_a = 0.8\ U_{ca} \tag{14}$$

where U_{ca} is the critical velocity corresponding to the d_{50a} particle size (calculated as described in Section 2.2). The first maximum scour depth therefore occurs at U_a (see Figure 2), and may be lower than for a uniform material if some of the finer sediment particles in the upstream bed are being transported. At higher flow velocities, the effect of armouring disappears and a second maximum scour depth occurs when the transitional flat-bed stage is reached. The behaviour of a non-uniform sediment is only different from a uniform one if its geometric standard deviation

$$\sigma_g = \frac{d_{84}}{d_{50}} > 1.3 \tag{15}$$

Based on these various findings, Melville & Sutherland (1988) developed the following design formula for estimating equilibrium scour depths at obstructions.

$$\frac{y_s}{B} = 2.4\ F_u\ (U'/U_c)\ .\ F_y(y_o/B)\ .\ F_d(d/B)$$

$$.\ F_s\ (\text{shape})\ .\ f_\alpha\ (\alpha,\ L/B) \tag{16}$$

This is similar in form to Breusers et al's Equation (7) but includes the effects of some additional factors. The flow velocity function F_u depends on the notional velocity

$$U' = U - (U_a - U_c) \tag{17}$$

where U is the mean flow velocity, U_a is the maximum velocity that can be resisted by a non-uniform sediment after armouring has occurred, and U_c is the critical velocity based on the d_{50} size of the original sediment mixture ; for a uniform sediment $U_a = U_c$. The function F_u is given by

$$F_u = | U'/U_c | \quad , \text{ for } U'/U_c \leq 1 \tag{18a}$$

$$F_u = 1 \text{ , for } U'/U_c > 1 \tag{18b}$$

The function F_y reduces the predicted scour if the flow depth y_o is less than 2.6B, and has the form

$$F_y = 0.78\ (y_o/B)^{0.255}, \text{ for } y_o/B \leq 2.6 \tag{19a}$$

$$F_y = 1 \text{ , for } y_o/B > 2.6 \tag{19b}$$

The sediment size was found not to influence the scour significantly unless the particle size exceeded approximately B/25. Beyond this limit, the scour depth was reduced because the particles were large enough to block the notched scour hole around the base of the obstacle (see Figure 1) and dissipate some of the energy of the associated down-flow. The function F_d is given by

$$F_d = 0.57 \log_{10}(2.24B/d_{50}), \text{ for } B/d_{50} \leq 25 \tag{20a}$$

$$F_d = 1.0 \text{ , for } B/d_{50} > 25 \tag{20b}$$

For live-bed scour and for a uniform material, the mean sediment size d_{50} should be used in Equation (20); for clear-water scour with a non-uniform sediment, the mean size of the armoured layer, d_{50a}, should be used.

The pier shape factor has a value of $F_s = 1.0$ for a circular cylinder ; values in the range $F_s = 1.11$ to 1.40 are suggested for rectangular piers. Melville & Sutherland recommend (like Breusers et al) the use of the data produced by Laursen & Toch (1953) on the effect of the angle of incidence ; for zero incidence, $f_\alpha = 1.0$.

Equation (16) is intended to produce conservative estimates of scour under all conditions, so the various functions described above represent envelope curves to the available data. According to Melville & Sutherland's Equation (16), the maximum possible scour depth for a circular cylinder is 2.4B, which compares with the figure of 2.0B given by the "design" version of Breusers et al's Equation (7).

3 EXPERIMENTAL ARRANGEMENT

3.1 Flume facility

All tests were carried out in a large flume facility having the dimensions:

Width	2.4 m
Depth	1.2 m
Length	28.0 m

Flow to the flume was provided by three centrifugal pumps having a combined total maximum discharge of 0.5 cumecs. Discharges were measured using orifice plates, conforming to British Standard 1042 Part 1 (1964), installed in all three pipe lines.

A false floor arrangement (see Figure 3) reduced the available depth of the flume to approximately 0.6m. The false floor created a working section where mobile bed material and piers of various shapes and sizes could be located.

Water levels in the flume were controlled using a fully adjustable tailgate, and levels could be monitored using tapping points located at the upstream and downstream ends of the test section.
Graduated rails were accurately levelled on the tops of both walls of the flume along the length of the test section. These were used, in conjunction with a cross-beam and a manually-operated point gauge, to survey the size and shape of the scour holes produced in the tests. Photographs taken by a camera mounted vertically above the test area were also used to aid the measurement of the horizontal extent of the scour holes.

Some time was spent at the beginning of the project on trials of an automatic bed-profiling machine for surveying the scour holes. The instrument used an optical head to traverse across the flume, but in its existing form it was not able to follow the steep sides of the scour holes. It therefore proved necessary to resort to the manual method of measurement described above.

Before the testing of any piers started, several horizontal velocity traverses and vertical velocity profiles were taken for flows with varying depths and discharges. This was carried out in order to establish that a uniform flow distribution existed in the region of the test area.

3.2 Choice of bed material

The study was specifically designed to investigate the effects of flow depth and structure size on the depth of scour. It was therefore decided to carry out the tests only under clear-water scour conditions (ie. $0.5 \leq U/U_c \leq 1.0$), and to avoid some of the complicating factors due to the sediment size and sediment grading described in Section 2.3.

The size of sediment used in the experiments was partly decided by the requirement that the achievable flow velocity in the flume at the maximum depth should not be less than the corresponding critical velocity U_c of the sediment. The available pumping capacity thus gave a limit of $U_c \leq 0.35$ m/s at a depth of $y_o = 0.6$ m. A quantity of quartz sand (Kings Lynn 100 supplied by British Industrial Sands) with a mean size of $d_{50} = 0.145$ mm was available, and was considered suitable as it was predicted to have a threshold velocity of about $U_c = 0.31$ m/s at $y_o = 0.6$ m. This sand had the advantage of a narrow grading, as shown in Figure 4 ; its principal characteristics were:

$d_{35} = 0.128$ mm
$d_{50} = 0.145$ mm
$d_{65} = 0.160$ mm
$d_{84} = 0.174$ mm
$d_{98} = 0.230$ mm
$\sigma_g = d_{84}/d_{50} = 1.20$
$s = 2.62$

The geometric standard deviation σ_g was below the limit of 1.3 given by Melville & Sutherland (1988), see Equation (15), so the grading could be considered as being effectively uniform ; complications due to the armouring of the bed were therefore avoided.

However, the sediment was fine enough to be subject to rippling when the flow velocity approached U_c. As described in Section 2.3, rippling can cause the maximum scour depth to be somewhat lower than would occur with a coarser uniform sediment. It was decided for this reason that most of the tests with different depths of flow and sizes of structure would be carried out at flow velocities below the general threshold of movement (see also Section 3.4).

Exploratory tests were carried out in a smaller 0.915m wide flume to determine values of the mean threshold velocity U_c for the Kings Lynn 100 sand under flat-bed conditions at flow depths of 0.05 m, 0.1 m and 0.2 m. The results are shown in Table 1, together with an estimate of U_c at a depth of 0.4 m obtained by curve-fitting and extrapolation. The measurements are also compared with predicted values of U_c given by Equations (5) and (6) and by the Shields curve (see Section 2.2). It can be seen that the measurements are in good agreement with Hanco's Equation (5) with a = 1.2.

3.3 Piers

Caissons and cofferdams used during the construction of bridges are the most common examples of obstructions that are large in relation to the depth of flow. Such structures are generally simple in shape, so it was decided to carry out the present study with vertical piers of square and circular cross-section. At the outset of the project, it was envisaged that piers with more complex geometries might also be studied, but this did not prove possible within the constraints imposed by budget and time.

The piers used in the study were required to be as large as possible, so an initial test was carried out in the 2.4 m wide flume with a square pier of side 0.80 m. This was found to cause too large a blockage in the flume because the flow patterns around the pier were adversely affected by the constriction. It was therefore decided to carry out tests on families of square and circular piers having widths of 0.40 m, 0.20 m and 0.10 m. The maximum size represented a blockage ratio of 1:6 which was considered satisfactory (Raudkivi & Ettema (1983) adopted a similar limit). The minimum pier size corresponded to a relative sediment ratio of B/d_{50} = 690 which was well outside the range within which sediment size might have been expected to influence the maximum scour depth (see Equation (20)). The square piers were always tested normal to the flow.

3.4 Experimental procedure

The layout of the flume and the mounting arrangement for the piers (see Figure 3) limited the depth of scour that could be allowed to about 0.4 m. Initial tests indicated that the maximum scour depths at the threshold condition $U = U_c$ would be of the same order as those found in previous studies, ie between 1.5 and 3 times the pier width. This, together with the desire to avoid rippling of the sediment bed (see Section 3.2), led to the decision to carry out most of the tests at a mean flow velocity of U = 0.18 m/s, corresponding to an average value of about U/U_c = 0.75. Tests were made using water depths of y_o = 0.40 m, 0.20 m, 0.10 m and 0.05 m. Rippling of the sediment bed occurred at the lowest depth, and made it difficult to measure the size of the scour hole accurately. Tests at this level were therefore carried out with a velocity of U = 0.17 m/s which was low enough to maintain a flat bed upstream of the pier.

The durations of the scour tests ranged from 44 hours to more than 70 hours. The maximum depths in the scour holes were measured regularly during the course of each test in order to help judge when an equilibrium condition had been reached. Increases in scour depth tended to occur very slowly towards the end of a test, so a decision about the equilibrium state necessarily had to be somewhat subjective. [Blaisdell (1988) has suggested that in fact no equilibrium condition exists and that scour may continue indefinitely at an infinitesimally small rate. However, a series of tests carried out over very long periods would not be very practicable, and the results would be of only theoretical interest since in nature steady flow conditions seldom persist for more than a few days].

At the end of each test, a detailed survey of the scour hole was made using the manually-operated point gauge and photographs were taken with a camera mounted above the flume.

4 TEST RESULTS AND ANALYSIS

4.1 Effect of flow velocity

For the reasons described in Section 3.4, it was decided to carry out the main scour tests at flow velocities below those needed for general bed movement. Separate tests were therefore made with a particular combination of pier size and water depth to study how the scour depth increased with flow velocity up to the threshold condition $U = U_c$. The water depth used was $y_o = 0.10$m, and five tests at different velocities were carried out with the 0.10m wide square pier and another four with the 0.10m diameter circular pier. The scour hole around a pier usually had two low points, one on either side of the pier. The scour depths y_{sl} and y_{sr} given in Table 2 refer to the left-hand side and right-hand side, respectively, of the pier when viewed from upstream.

Figures 5a and b show in non-dimensional form how the scour depth varied with flow velocity for the square and circular piers. It can be seen in the case of the square pier (Figure 5a) that a well-defined linear relationship exists between the ratios y_s/y_{sc} and U/U_c, where y_{sc} is the scour depth at the critical velocity U_c. The equation of the best-fit line is

$$\text{square pier : } \frac{y_s}{y_{sc}} = 1.6 \frac{U}{U_c} - 0.6 \qquad (21)$$

$$\text{for } 0.375 \le U/U_c \le 1.0$$

In the case of the circular pier, a curved relationship applies and this can be approximated by

$$\text{circular pier : } \frac{y_s}{y_{sc}} = 1 - 3.66 \left(1 - \frac{U}{U_c}\right)^{0.76} \qquad (22)$$

$$\text{for } 0.52 \le U/U_c \le 1.0$$

which is shown plotted in Figure 5b. Also included are lines corresponding to Equation (8b) which is used in Breusers et al's Equation (7), and Equation (18a) which is used in Melville & Sutherland's Equation (16); in the latter case the sediment is assumed to be uniform so that $U_a = U_c$. The comparisons show that Melville & Sutherland's equation overestimates the scour, particularly at low velocities, while Breusers et al's equation underestimates it, particularly in the case of circular cylinders in the velocity range $0.7 < U/U_c < 0.9$.

4.2 Effects of pier size and flow depth

The main scour tests were carried out using three square and three circular piers in four different depths of water. The values of relative flow depth y_o/B studied with the square piers are shown in the following matrix.

		Pier width B (m)		
		0.40	0.20	0.10
water depth y_o (m)	0.40	1.00	2.00	4.00
	0.20	0.50	1.00	2.00
	0.10	0.25	0.50	1.00
	0.05	0.125	0.25	0.50

In the case of the circular piers, attention was concentrated on the smaller values of y_o/B and the corresponding test matrix was as follows.

		Pier diameter B (m)		
		0.40	0.20	0.10
water depth y_o (m)	0.40	1.00	-	-
	0.20	0.50	1.00	-
	0.10	0.25	-	1.00
	0.05	0.125	0.25	0.50

As described in Section 3.4, the tests were carried out at a flow velocity of about 0.18 m/s, except in the case of the lowest water depth (y_o= 0.05m) where it proved necessary to reduce the velocity slightly to about 0.17 m/s. Table 3 gives for each test : the exact value of the mean flow velocity U ; the flow ratio U/U_c; the depths of scour y_{sl} and y_{sr} on the left-hand and right-hand sides of the pier at the end of the test ; the mean value y_s of y_{sl} and y_{sr} ; and the duration D of the test. Test C.7 with the 0.40 m diameter pier was unusual in that there was a significant difference in scour depths between the two sides of the pier. The test was therefore repeated as number C.7R ; the scour holes remained asymmetric but the deeper scour now occurred on the right-hand instead of the left-hand side.

Data on the development of the scour holes with time are given in Table 4. Some previous researchers have fitted such data to an exponential equation of the form

$$\frac{y_t}{y_s} = 1 - \exp(-ct^{\gamma}) \tag{23}$$

where y_t is the scour depth at time t and y_s is the equilibrium scour depth. If such an equation were valid, it could be used to estimate the ultimate scour depth from measurements obtained over a limited period. Unfortunately, the data in Table 4 did not fit Equation (23) with constant values of the coefficients c and γ, so such an extrapolation was not considered justified. The analysis described in Section 4.3 was therefore based on the scour depths measured at the end of each test.

The scour patterns obtained at the ends of Tests S.6 to S.17 and C.5 to C.13 are shown in contour form in Figures 6 to 26. The scour holes around the square piers were usually almost symmetrical and were deepest at the two upstream corners. In the case of the circular piers, the maximum scour depths occurred towards the sides and tended to be somewhat less symmetrical ; this was probably because the points of flow separation were able to shift as the scour holes developed. Comparison of the Figures indicates that geometric scaling is valid over the range of conditions investigated in this study. Thus, tests with different sizes of pier produced similar shapes of scour hole ; also the ratios between the size of the pier and the dimensions of the scour hole remained approximately constant. This can be seen, for example, by comparing Figures 6, 11 and 16 for square piers with a relative flow depth of $y_o/B = 1.00$; Figures 7, 12 and 17 for $y_o/B = 0.50$; and Figures 18, 23 and 25 for circular piers at $y_o/B = 1.00$.

4.3 Analysis

The purpose of the following analysis was to identify from the test results how the depth of scour varied with pier size and flow depth. The scour data in Table 3 could not be compared directly because the tests at different water depths were carried out with different values of the flow ratio U/U_c. The first step therefore was to scale the results so as to predict values of the scour depth y_{sc} at the critical threshold condition $U = U_c$. As explained in Section 4.1, separate best-fit relationships were established between y_s/y_{sc} and U/U_c for the square pier (Equation (21)) and the circular pier (Equation (22)), based on the measurements obtained with the 0.10m wide piers in a water depth of 0.10m. Similar types of curves have been obtained by previous researchers for different ratios of pier size to water depth, and it seems reasonable to assume that Equations (21) and (22) can be applied to the other tests carried out in this study. Table 3 therefore gives calculated values of the ratio y_{sc}/B, where the measured scour depth y_s (equal to the mean of y_{sl} and y_{sr} on either side of the pier) was scaled up, using either Equation (21) or (22), to give the value of y_{sc} at $U=U_c$.

The values of y_{sc}/B for the square piers are plotted against the relative flow depth y_o/B in Figure 27a. It can be seen that the results obtained with different pier sizes at the same flow depth ratio agree reasonably well, and suggest that geometric scaling is valid over the range of conditions studied. An unexpected feature is that the value of y_{sc}/B does not level off at a value of $y_o/B = 1 - 2$, as found by some previous researchers, but continues to increase up to about $y_o/B = 3 - 4$. The corresponding set of results for the circular piers is shown in Figure 27b.

These cover only relative flow depths up to y_o /B = 1.0, but again there is no evidence of a levelling off in the value of y_{sc}/B at this limit.

Comparison of Figures 27a and b shows that, for equal values of relative flow depth, the square piers experienced greater scour depths than the circular ones. The mean ratios between the scour depths for the two pier shapes were

y_o/B	y_{sc}(square)/y_{sc}(circular)
0.125	1.70
0.25	1.54
0.50	1.46
1.00	1.20

The overall mean value of the ratio (taking into account the number of points) was 1.33, which is in reasonable agreement with other studies (eg f_s = 1.3 in Breusers et al's Equation (7) and F_s = 1.11 to 1.4 in Melville & Sutherland's Equation (16)). Accepting this mean figure of 1.33, it was then possible to analyse on a common basis the two sets of data for the square and circular piers.

In order to determine by how much the depth of scour was reduced by shallow-water effects, it was first necessary to estimate the maximum scour depth, y_{sm}, which would occur in deep water. As explained above, the effect of relative flow depth extended to higher levels than expected, so data were available from only three tests with $y_o/B \geq 2$. The largest scour ratio measured was y_s/B = 3.19 for the square pier at y_o/B = 4. According to Melville & Sutherland (1988), the maximum value of the scour ratio for a square pier in deep water can be expected to be in the range 2.7

to 3.4 (depending on the assumed value of the shape factor F_s in Equation (16)). This suggests that the scour recorded in the test at $y_o/B = 4$ was close to the maximum value which would occur in deep water. The following analysis was therefore carried out assuming maximum values of $y_{sm}/B = 3.2$ for square piers and $y_{sm}/B = 2.4$ for circular piers; these figures are consistent with the mean shape factor of 1.33 (square/circular) and also with Equation (16) for circular piers.

The required function describing the effect of relative depth was obtained by dividing the values of y_{sc}/B by the corresponding ratios of y_{sm}/B given above. All the data for the square and circular piers are plotted in the form of y_{sc}/y_{sm} versus y_o/B in Figure 28. The vertical line and circle at each value of y_o/B indicate, respectively, the range of the data and the mean value; the individual data points are listed in Table 5. The equation of the best-fit curve in Figure 28 is

$$\frac{y_{sc}}{y_{sm}} = 0.44\,(y_o/B)^{0.67}\ , \text{ for } y_o/B \leqslant 3.4 \qquad (24)$$

For $y_o/B > 3.4$, the ratio $y_{sc}/y_{sm} = 1$
Also shown in Figure 28 is the envelope curve to all the data in the present study, which has the equation

$$\frac{y_{sc}}{y_{sm}} = 0.55\,(y_o/B)^{0.60}, \text{ for } y_o/B \leqslant 2.7 \qquad (25)$$

These curves are compared with the depth functions proposed by Breusers et al (from equation (7)) :

$$\frac{y_{sc}}{y_{sm}} = \tanh\,(y_o/B) \qquad ; \qquad (26)$$

by Torsethaughen (from Equation (12) assuming $y_{sm}/B = 2.4$):

$$\frac{y_{sc}}{y_{sm}} = 0.345 \; (y_o/B)$$

$$, \text{ for } 0.2 \leq y_o/B \leq 0.65; \qquad (27)$$

and by Melville & Sutherland (from Equation (19a))

$$\frac{y_{sc}}{y_{sm}} = 0.78 \; (y_o/B)^{0.255}, \text{ for } y_o/B \leq 2.6 \qquad (28)$$

Equation (27) underestimates the scour depths obtained in the present study, but it relies on an assumption about the deep-water scour ratio y_{sm}/B, the value of which was not determined.

Equations (26) and (28) appear to significantly overestimate the depth of scour that occurs when the size of an obstruction is large in relation to the depth of flow. In the case of structures such as bridge cofferdams, which can typically have widths between 10m and 15m, the differences in the predicted scour depths can be substantial in absolute terms. Equation (25), which provides safe estimates for all the tests in the present study, is proposed as a suitable method for predicting scour depths around large obstructions.

The results of the present study can therefore be summarised in the following prediction formula

$$y_s = 2.4 \; f_s \; (y_s/y_{sc}) \cdot (y_{sc}/y_{sm}) \qquad (29)$$

where for a circular cylinder $f_s = 1.0$ and

$$\frac{y_s}{y_{sc}} = 1 - 3.66 \left(1 - \frac{U}{U_c}\right)^{1.76} \qquad (22)$$

$$, \text{ for } 0.52 \le U/U_c \le 1.0,$$

and $y_s/y_{sc} = 1.0$ when $U/U_c > 1.0$.

Methods of predicting the critical velocity U_c are given in section 2.2. Hanco's Equation (5) with a value of a = 1.2 was found to give satisfactory results in this study, and compares reasonably with other formulae when used with larger flow depths and sediment sizes.

For a square pier at zero angle of incidence $f_s = 1.33$ and

$$\frac{y_s}{y_{sc}} = 1.6 \frac{U}{U_c} - 0.6 \qquad (21)$$

$$, \text{ for } 0.375 \le \frac{U}{U_c} \le 1.$$

and $y_s/y_{sc} = 1.0$ when $U/U_c > 1.0$.

Equation (21) can also be expected to apply to rectangular piers in line with the flow. For both square and circular piers, the value of y_{sc}/y_{sm} is determined from Equation (25) ; $y_{sc}/y_{sm} = 1.0$ when $y_o/B > 2.7$.

5 CONCLUSIONS

1. Scour tests were carried out using square and circular piers with widths of B = 0.1m, 0.2m and 0.4m. The relative flow depths studied with the square piers were y_o/B = 0.125, 0.25, 0.50, 1.0, 2.0 and 4.0, and with the circular piers they were y_o/B = 0.125, 0.25, 0.50 and 1.0. The square piers were always tested normal to the flow.

2. The effect of flow velocity on scour depth was studied using 0.1m wide square and circular piers

with a flow depth of $y_o = 0.1m$. With the square pier, a linear relationship was established between scour depth and velocity (Equation (21)); with the circular pier, the relationship was non-linear (Equation (22)).

3. For given flow conditons, the depth of scour at a square pier (at zero angle of incidence) was on average 1.33 times the depth at a circular pier of equal width.

4. The effect of relative flow depth y_o/B on the scour depth is shown in Figure 28. The maximum depth of scour in deep water, y_{sm}, was estimated to be equal to 3.2 B for square piers and 2.4 B for circular piers. The best-fit curve describing the effect of relative flow depth is given by Equation (24). The upper envelope to the data in Figure 28 is given by Equation (25), which provides conservative estimates of scour relative to all the tests in the present study.

5. The results of the study are summarised by Equations (29), (25), (22) and (21), which are recommended for estimating scour depths around large obstructions in shallow water. When $y_o/B < 1$, these equations predict significantly smaller scour depths than Breusers et al's Equation (7) and Melville & Sutherland's Equation (16).

6 ACKNOWLEDGEMENTS

The experimental work was carried out by Mr I R Willoughby who also assisted with the analysis. The project was supervised by Mr J A Perkins and Mr R W P May, and was carried out in the River Engineering Department headed by Dr W R White.

7 REFERENCES

ACKERS P & WHITE W R (1973). Sediment transport: a new approach and analysis. Jnl Hydr Div, Amer Soc Civ Engrs, Vol 99, No 11, pp 2041-2060.

BLAISDELL F W (1988). Discussion of: Do critical stresses for incipient motion and erosion really exist? by W Lavelle & H O Mofjeld. Jnl Hydr Engng, Amer Soc Civ Engrs, Vol 114, No 8, pp 960-963.

BREUSERS H N C, NICOLLET G & SHEN H W (1977). Local scour around cylindrical piers. Jnl Hydr Res, Vol 15, No 3, pp 211-252.

BRITISH STANDARDS INSTITUTION (1964). Methods for the measurement of fluid flow in pipes. Part 1: Orifice plates, nozzles and venturi tubes. British Standard 1042.

CARSTENS T & SHARMA H R (1975). Local scour around large obstructions. Proc 16th IAHR Congress, Sao Paulo, Vol 2, pp 251-262.

CHIEW Y M & MELVILLE B W (1989). Local scour at bridge piers with non-uniform sediments. Proc Inst Civ Engrs, Part 2, Vol 87, June, pp 215-224.

HANCO S (1971). Sur le calcul des affouillements locaux dans la zone des piles de ponts. Proc 14th IAHR Congress, Paris, Vol 3, pp 299-313.

HENDERSON F M (1966). Open Channel Flow. The Macmillan Company, New York.

LAURSEN E M & TOCH A (1956). Scour around bridge piers and abutments. Iowa Highway Research Board, Bull No 4.

MELVILLE B W (1984). Live-bed scour at bridge piers. Jnl Hydr Engng, Amer Soc Civ Engrs, Vol 110, No 9, pp 1234-1247.

MELVILLE B W & SUTHERLAND A J (1988). Design method for local scour at bridge piers. Jnl Hydr Engng, Amer Soc Civ Engrs, Vol 114, No 10, pp 1210-1226.

RAUDKIVI A J (1986). Functional trends of scour at bridge piers. Jnl Hydr Engng, Amer Soc Civ Engrs, Vol 112, No 1, pp 1-13.

RAUDKIVI A J & ETTEMA R (1983). Clear-water scour at cylindrical piers. Jnl Hydr Engrs, Amer Soc Civ Engrs, Vol 109, No 3, pp 338-350.

SHEN H W, SCHNEIDER V R & KARAKI S (1966). Mechanics of local scour. Colorado State Univ, CER 66 HWS-VRS-SK22.

TORSETHAUGEN K (1975). Lokalerosjon ved store konstruksjoner Modellforsok. Vassdrago-og Havnelaboratoriet, Trondheim (in Norwegian).

TABLES

TABLE 1 : MEASURED AND PREDICTED THRESHOLD VELOCITIES

FLOW DEPTH Y_o (m)	THRESHOLD VELOCITY Uc (m/s)			
	OBSERVED	PREDICTED BY :		
	HRL FLUME TESTS	HANCO Eqn (5)	SHIELDS Eqns (1) & (2)	ACKERS-WHITE Eqn (6)
0.050	0.192	0.191	0.224	0.251
0.100	0.235	0.219	0.245	0.272
0.200	0.254	0.252	0.266	0.293
0.400	** 0.298	0.289	0.286	0.314

** VALUE ESTIMATED BY CURVE FITTING AND EXTRAPOLATION

TABLE 2 : VARIATION OF SCOUR DEPTH WITH VELOCITY

DATA FOR SQUARE PIERS

TEST CODE NUMBER	PIER WIDTH B (m)	FLOW DEPTH Y_o (m)	VELOCITY U (m/s)	$\frac{U}{U_c}$	SCOUR DEPTHS(m) Y_{sl}	Y_{sr}	Y_s	$\frac{Y_{sc}}{B}$ ‡
S1	0.10	0.10	0.103	0.429	0.011	0.011	0.011	1.273
S2	0.10	0.10	0.129	0.538	0.032	0.046	0.039	1.495
S3	0.10	0.10	0.175	0.729	0.070	0.071	0.071	1.254
S4	0.10	0.10	0.184	0.767	0.082	0.080	0.081	1.291
S5	0.10	0.10	0.240	1.000	0.140	0.140	0.140	1.400
S16	0.10	0.10	0.183	0.763	0.096	0.091	0.094	1.514

DATA FOR CIRCULAR PIERS

TEST CODE NUMBER	PIER WIDTH B (m)	FLOW DEPTH Y_o (m)	VELOCITY U (m/s)	$\frac{U}{U_c}$	SCOUR DEPTHS(m) Y_{sl}	Y_{sr}	Y_s	$\frac{Y_{sc}}{B}$ ‡
C1	0.10	0.10	0.123	0.513	0.006	0.008	0.007	-
C2	0.10	0.10	0.139	0.579	0.020	0.020	0.020	0.999
C3	0.10	0.10	0.177	0.738	-	0.075	0.075	1.150
C4	0.10	0.10	0.237	0.988	0.126	0.124	0.125	1.252
C11	0.10	0.10	0.183	0.763	0.092	0.091	0.092	1.298

‡ ESTIMATED VALUES

TABLE 3 : VARIATION OF SCOUR DEPTH WITH PIER WIDTH AND FLOW DEPTH

TEST DATA FOR SQUARE PIERS

TEST CODE NUMBER	PIER WIDTH B (m)	FLOW DEPTH Y_o (m)	VELOCITY U (m/s)	$\frac{U}{U_c}$	SCOUR DEPTHS (m) Y_{sl}	Y_{sr}	Y_s	$\frac{Y_{sc}}{B}$ *	D (hrs)
S6	0.40	0.40	0.183	0.610	0.223	0.212	0.218	1.449	60.25
S7	0.40	0.20	0.183	0.732	0.220	0.206	0.213	0.932	74.25
S8	0.40	0.10	0.183	0.763	0.172	0.165	0.169	0.681	53.50
S9	0.40	0.05	0.171	0.900	0.107	0.106	0.107	0.318	52.50
S10	0.20	0.40	0.183	0.610	0.158	0.165	0.162	2.154	54.25
S11	0.20	0.20	0.183	0.732	0.152	0.152	0.152	1.331	47.50
S12	0.20	0.10	0.183	0.763	0.124	0.132	0.128	1.031	50.50
S13	0.20	0.05	0.171	0.900	0.080	0.080	0.080	0.476	54.25
S14	0.10	0.40	0.183	0.610	0.117	0.123	0.120	3.191	48.25
S15	0.10	0.20	0.183	0.732	0.114	0.114	0.114	1.996	54.00
S16	0.10	0.10	0.183	0.763	0.096	0.091	0.094	1.514	48.00
S17	0.10	0.05	0.183	0.963	0.062	0.068	0.065	0.691	53.00

TEST DATA FOR CIRCULAR PIERS

TEST CODE NUMBER	PIER WIDTH B (m)	FLOW DEPTH Y_o (m)	VELOCITY U (m/s)	$\frac{U}{U_c}$	SCOUR DEPTHS (m) Y_{sl}	Y_{sr}	Y_s	$\frac{Y_{sc}}{B}$ *	D (hrs)
C5	0.40	0.40	0.183	0.610	0.142	0.141	0.142	1.181	72.25
C6	0.40	0.20	0.183	0.732	0.136	0.122	0.129	0.505	71.75
C7	0.40	0.10	0.183	0.763	0.127	0.100	0.114	0.402	76.00
C7R	0.40	0.10	0.183	0.763	0.100	0.113	0.107	0.377	57.00
C8	0.40	0.05	0.171	0.900	0.083	0.057	0.070	0.187	53.75
C9	0.20	0.20	0.183	0.732	0.126	0.132	0.129	1.011	52.75
C10	0.20	0.05	0.171	0.900	0.070	0.060	0.065	0.347	52.50
C11	0.10	0.10	0.183	0.763	0.091	0.092	0.092	1.298	44.50
C12	0.10	0.05	0.171	0.900	0.065	0.067	0.066	0.705	44.25

* ESTIMATED VALUES

TABLE 4 : VARIATION OF SCOUR DEPTH WITH TIME

SQUARE PIERS

TEST S6 TIME	SCOUR DEPTH	TEST S7 TIME	SCOUR DEPTH	TEST S8 TIME	SCOUR DEPTH	TEST S9 TIME	SCOUR DEPTH	TEST S10 TIME	SCOUR DEPTH	TEST S11 TIME	SCOUR DEPTH
3.00	127.0	0.25	50.0	0.50	77.5	0.50	28.5	0.75	75.0	0.50	60.0
7.00	155.0	0.50	60.0	1.00	104.5	1.00	43.5	2.25	113.5	2.50	107.0
26.50	197.5	1.00	80.0	1.50	110.0	1.75	53.0	3.75	127.5	4.00	110.0
30.75	201.0	1.25	90.0	2.50	118.0	4.00	60.0	5.25	130.5	6.00	111.0
35.75	208.0	1.75	100.0	5.25	126.5	4.75	70.5	6.75	132.5	22.50	125.0
60.25	218.0	2.25	100.0	6.00	128.0	21.00	73.5	22.75	147.5	25.00	130.0
		2.75	100.0	22.00	149.0	24.50	93.5	25.75	151.0	27.50	131.5
		3.25	105.0	24.50	154.5	28.50	99.5	28.25	154.0	30.00	135.0
		20.25	150.0	27.50	156.0	45.00	101.0	30.25	156.0	40.50	143.0
		22.25	155.0	29.50	159.0	50.00	105.5	46.75	156.0	43.00	147.0
		23.25	156.5	46.25	164.5	52.50	106.5	50.00	158.5	45.50	150.0
		25.25	157.5	53.50	168.5			52.00	162.0	47.50	152.0
		26.25	170.0					54.25	161.5		
		27.25	170.0								
		44.75	197.5								
		46.75	202.5								
		67.75	213.5								
		74.25	213.0								

TEST S12 TIME	SCOUR DEPTH	TEST S13 TIME	SCOUR DEPTH	TEST S14 TIME	SCOUR DEPTH	TEST S15 TIME	SCOUR DEPTH	TEST S16 TIME	SCOUR DEPTH	TEST S17 TIME	SCOUR DEPTH
1.00	60.0	0.50	27.5	0.50	56.5	0.50	54.5	0.75	54.0	0.50	41.0
2.25	85.0	1.50	38.0	1.00	67.0	1.50	78.0	2.75	57.5	1.50	47.0
3.75	105.0	2.00	55.5	3.00	76.0	2.25	83.0	5.25	61.5	2.75	50.0
21.25	119.0	3.75	59.0	4.75	81.5	4.00	91.0	7.00	65.0	5.50	51.0
24.25	123.0	5.00	61.0	21.75	101.0	5.50	91.5	23.00	80.5	21.75	59.0
28.50	128.0	6.25	64.0	24.25	102.0	22.50	99.0	25.25	84.0	24.00	61.0
31.50	132.0	22.75	68.0	26.75	108.0	25.00	101.0	26.75	84.0	25.50	62.0
50.50	128.0	25.50	68.0	30.00	109.5	27.75	102.5	28.25	85.0	28.00	62.5
		28.50	69.0	45.75	114.5	30.50	103.0	29.75	85.0	29.75	62.5
		30.50	72.5	48.25	120.0	46.50	107.0	30.75	87.0	45.50	65.0
		46.75	75.0			54.00	114.0	46.75	91.0	48.00	65.0
		54.25	80.0					48.00	94.0	53.00	65.0

CIRCULAR PIERS

TEST C5 TIME	SCOUR DEPTH	TEST C6 TIME	SCOUR DEPTH	TEST C7 TIME	SCOUR DEPTH	TEST C7R TIME	SCOUR DEPTH
0.50	28.0	0.50	35.0	0.50	24.5	0.50	27.0
2.25	41.5	2.00	43.5	1.50	39.0	1.00	38.0
3.25	47.5	3.00	48.5	3.25	48.0	2.00	42.5
19.00	110.0	5.75	53.0	20.25	78.0	2.50	46.0
21.00	110.5	7.00	61.5	23.25	83.0	19.00	74.5
23.25	118.0	23.25	120.0	26.50	86.0	21.25	75.0
25.50	118.5	25.25	122.5	28.25	86.0	24.25	81.5
43.25	132.0	27.50	124.5	44.25	101.5	26.50	82.0
46.00	135.0	31.00	124.5	47.25	105.5	28.25	84.5
49.50	138.0	47.25	133.0	49.75	105.5	29.75	86.5
67.00	141.5	49.75	133.0	52.25	106.5	32.75	89.0
72.25	142.0	71.75	129.0	68.25	114.0	33.75	92.0
				70.75	113.5	50.75	107.0
				74.75	116.0	53.75	112.0
				76.00	113.5	57.00	106.5

TEST C8 TIME	SCOUR DEPTH	TEST C9 TIME	SCOUR DEPTH	TEST C10 TIME	SCOUR DEPTH	TEST C11 TIME	SCOUR DEPTH	TEST C12 TIME	SCOUR DEPTH
0.50	20.0	0.50	19.0	0.50	17.0	0.75	33.5	0.50	12.0
1.00	24.0	1.75	30.5	1.00	21.0	1.25	39.0	1.25	15.0
1.50	25.5	2.75	54.5	2.00	27.0	2.00	44.5	3.00	27.0
2.25	32.0	4.25	64.0	3.00	30.0	3.00	48.5	4.00	32.0
3.75	37.5	6.25	73.5	4.50	34.5	5.25	64.0	20.75	57.5
4.50	39.5	22.75	102.5	21.25	56.5	20.50	80.5	23.00	58.0
5.75	41.0	26.75	107.5	24.25	62.0	24.50	83.5	26.75	61.0
22.50	39.0	29.75	112.5	26.75	61.0	29.00	86.0	44.25	66.0
25.50	42.0	47.25	124.0	28.75	62.5	44.50	91.5		
27.50	43.0	50.25	126.5	45.00	62.0				
29.75	45.0	52.75	129.0	48.00	64.5				
46.25	67.5			52.50	65.0				
53.75	70.0								

Note :- Scour Depth in mm ; Time in hours

TABLE 5 : ANALYSED DATA FOR RELATIVE FLOW DEPTH

TEST CODE NUMBER	y_o (m)	B (m)	$\frac{y_o}{B}$	$\frac{y_{sc}}{y_{sm}}$
S14	0.40	0.10	4.00	0.997
S10	0.40	0.20	2.00	0.673
S15	0.20	0.10	2.00	0.624
S6	0.40	0.40	1.00	0.453
S11	0.20	0.20	1.00	0.416
S16	0.10	0.10	1.00	0.473
S1	0.10	0.10	1.00	0.398
S2	0.10	0.10	1.00	0.467
S3	0.10	0.10	1.00	0.392
S4	0.10	0.10	1.00	0.403
S5	0.10	0.10	1.00	0.438
C5	0.40	0.40	1.00	0.492
C9	0.20	0.20	1.00	0.421
C11	0.10	0.10	1.00	0.541
C2	0.10	0.10	1.00	0.416
C3	0.10	0.10	1.00	0.479
C4	0.10	0.10	1.00	0.522
S7	0.20	0.40	0.50	0.291
S12	0.10	0.20	0.50	0.322
S17	0.05	0.10	0.50	0.216
C6	0.20	0.40	0.50	0.210
C12	0.05	0.10	0.50	0.294
S8	0.10	0.40	0.25	0.213
S13	0.05	0.20	0.25	0.149
C7	0.10	0.40	0.25	0.168
C7R	0.10	0.40	0.25	0.157
C10	0.05	0.20	0.25	0.145
S9	0.05	0.40	0.125	0.099
C8	0.05	0.40	0.125	0.078

FIGURES.

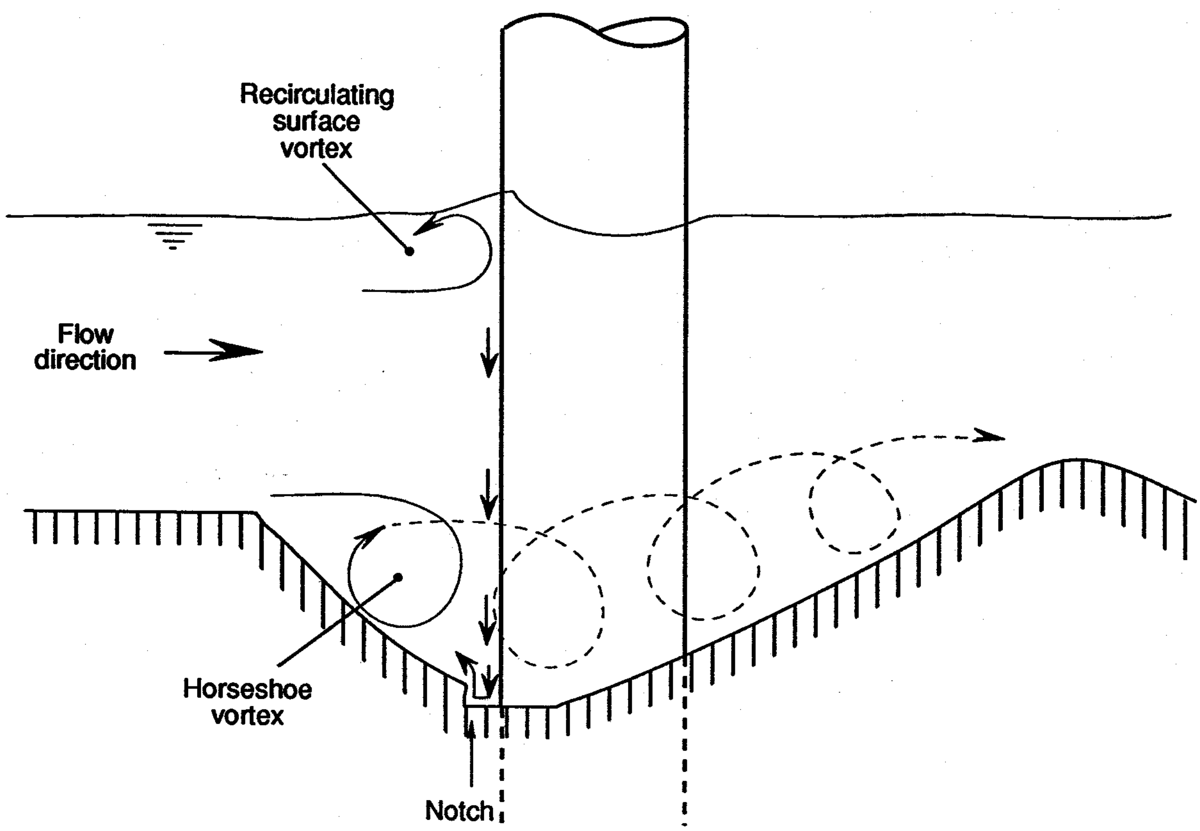

Fig 1 Diagrammatic representation of flow pattern at an obstruction

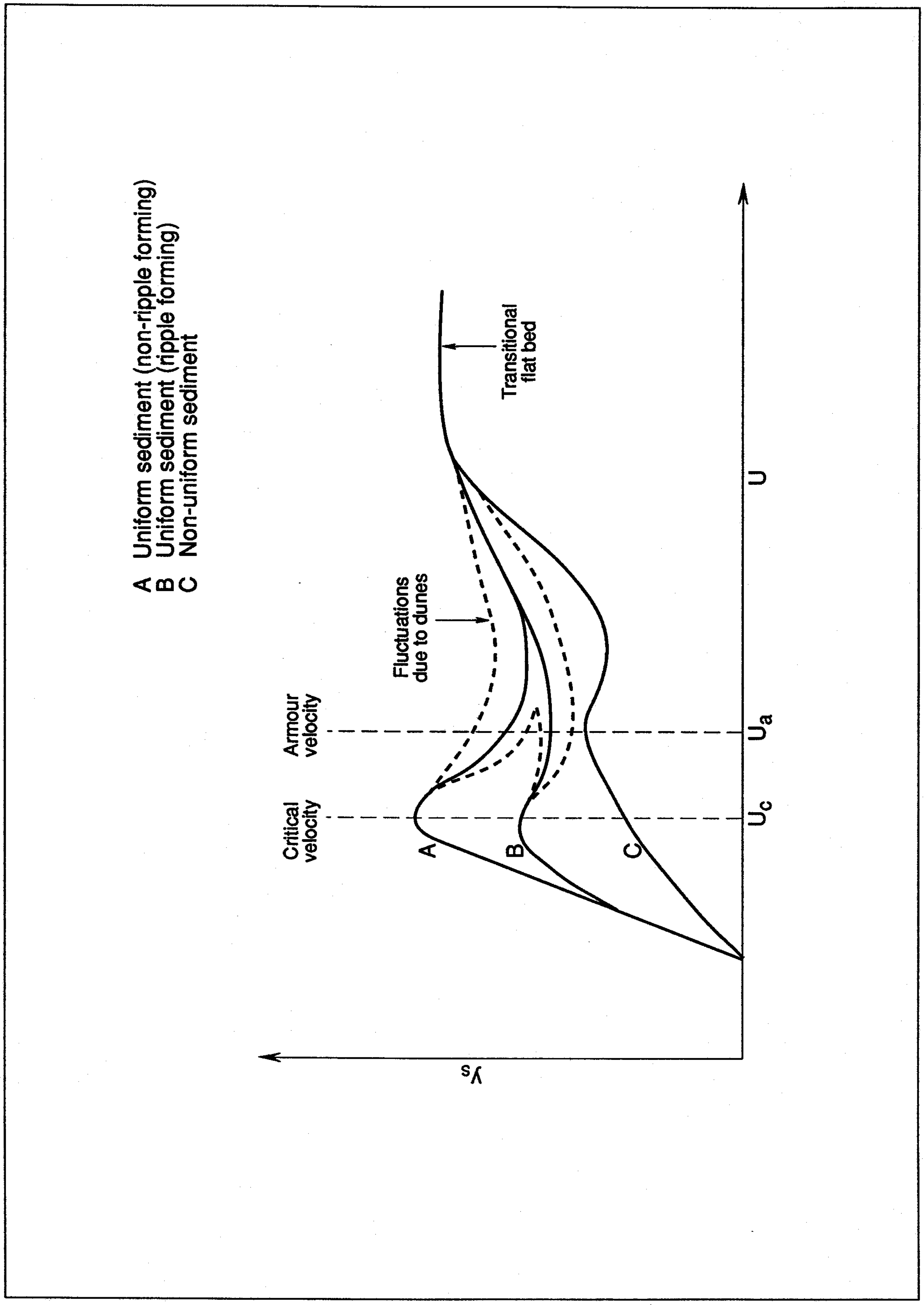

Fig 2 Variation of scour depth with velocity for different sediments

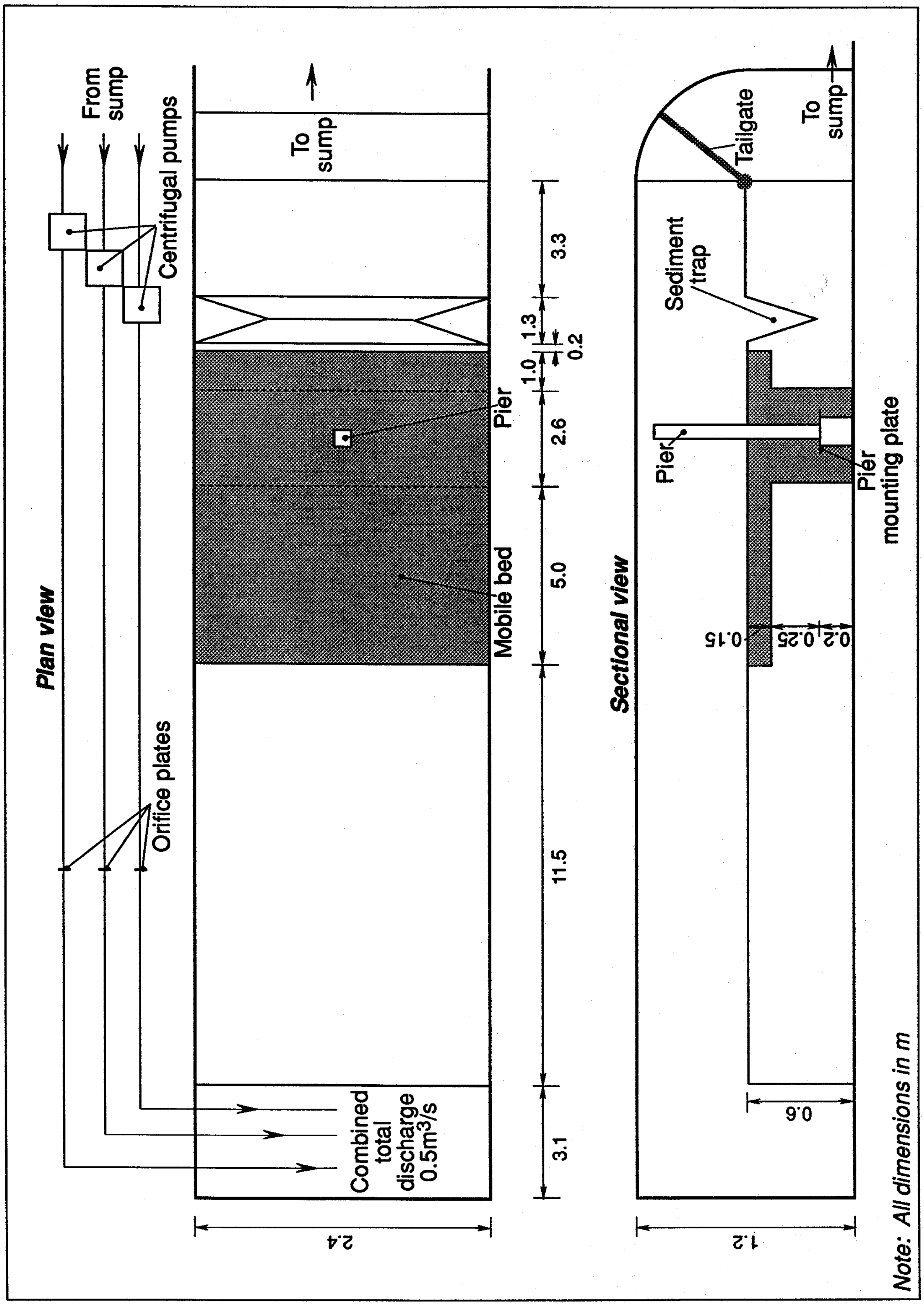

Fig 3 Layout of flume facility

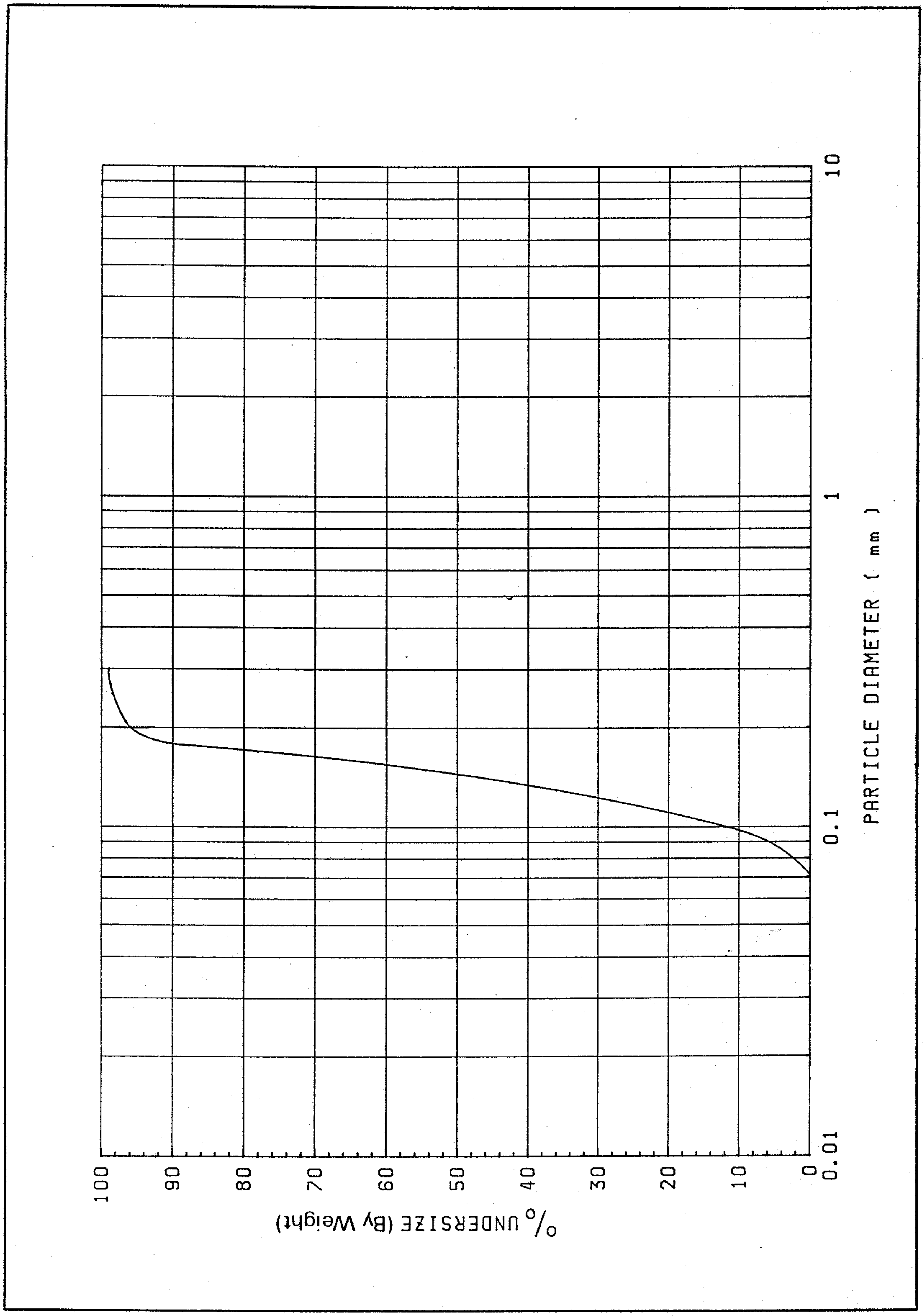

FIG 4 SIZE GRADING OF SEDIMENT

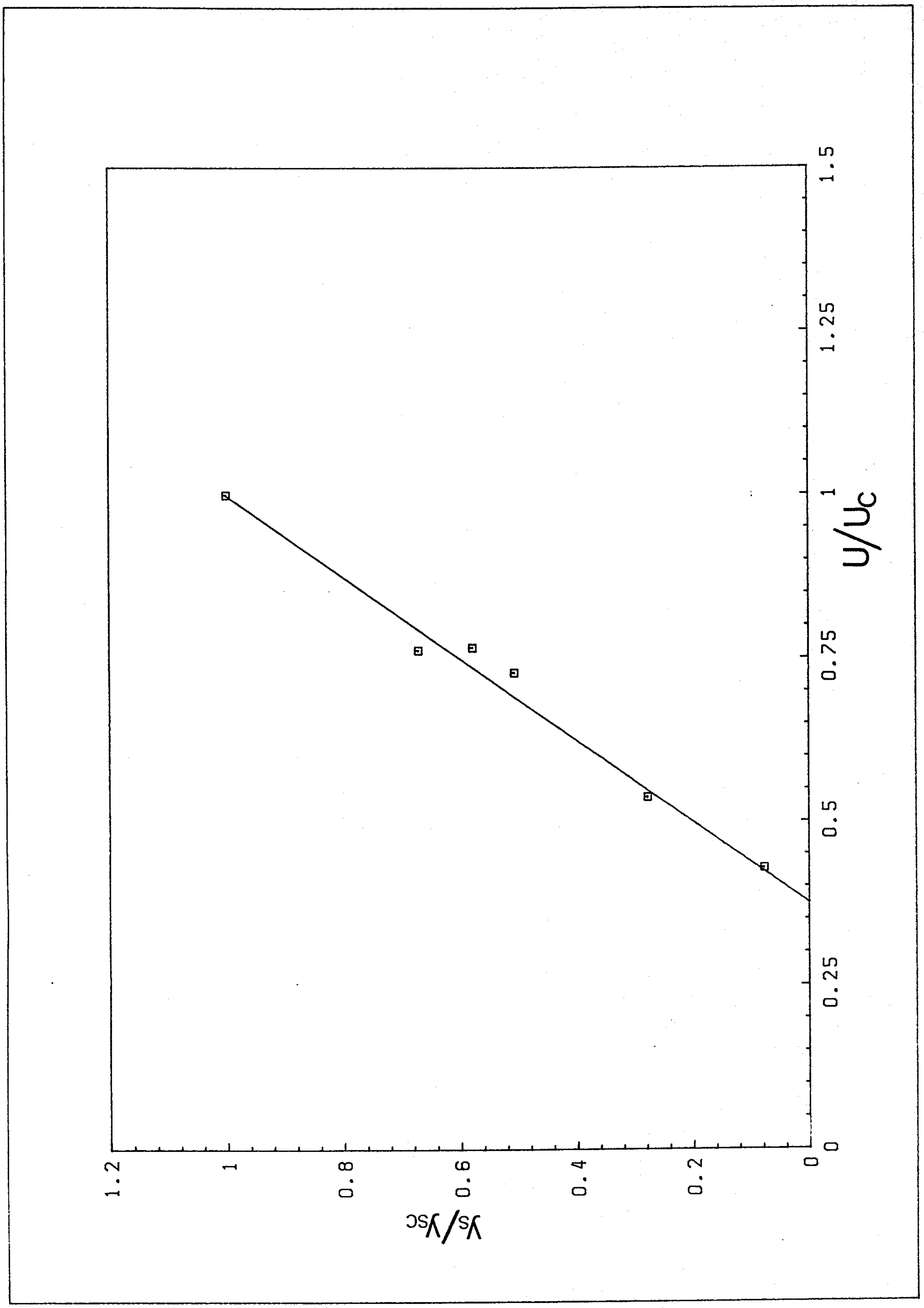

FIG 5a VARIATION OF SCOUR DEPTH WITH FLOW VELOCITY
FOR SQUARE PIERS

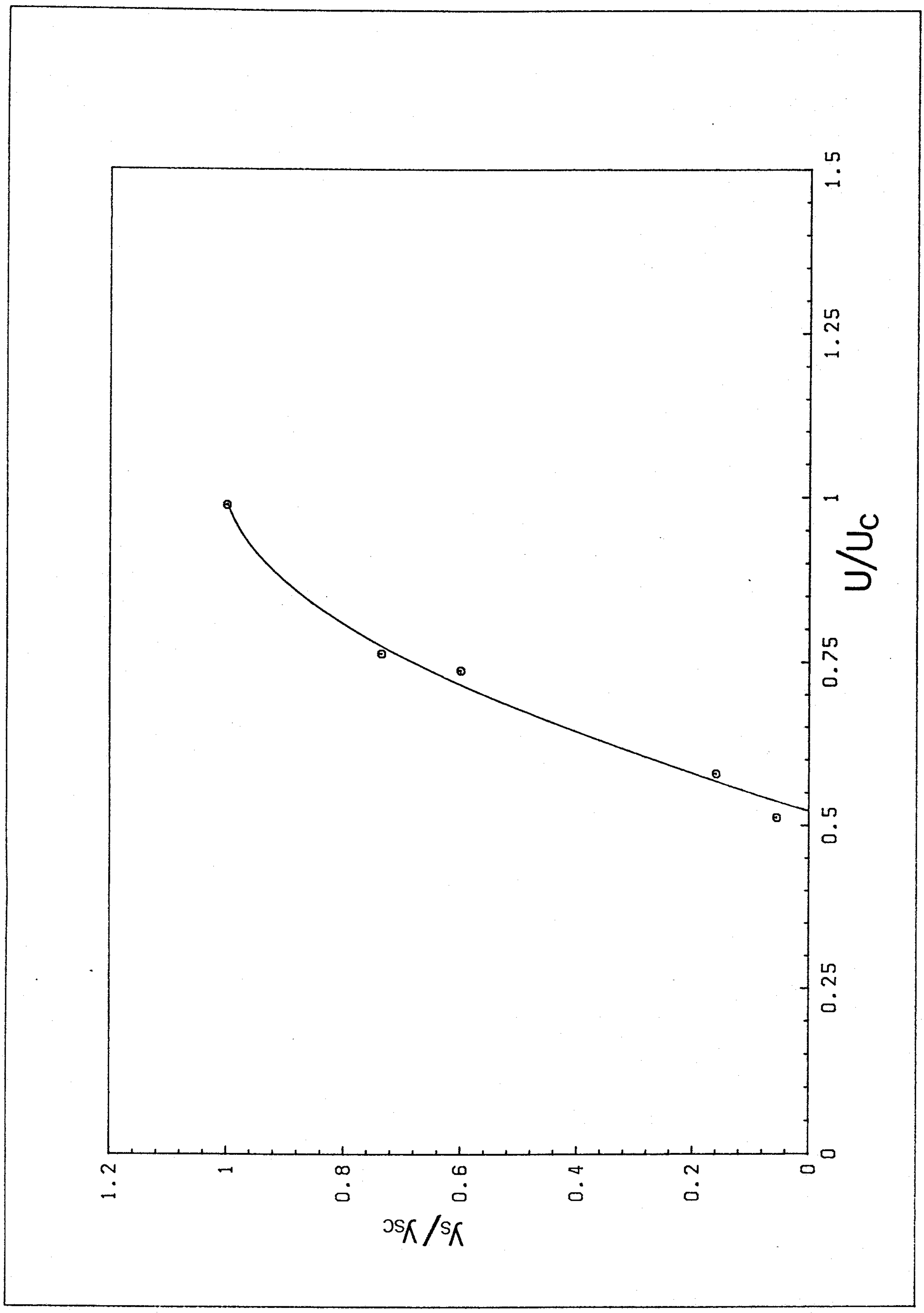

FIG 5b   VARIATION OF SCOUR DEPTH WITH FLOW VELOCITY
FOR CIRCULAR PIERS

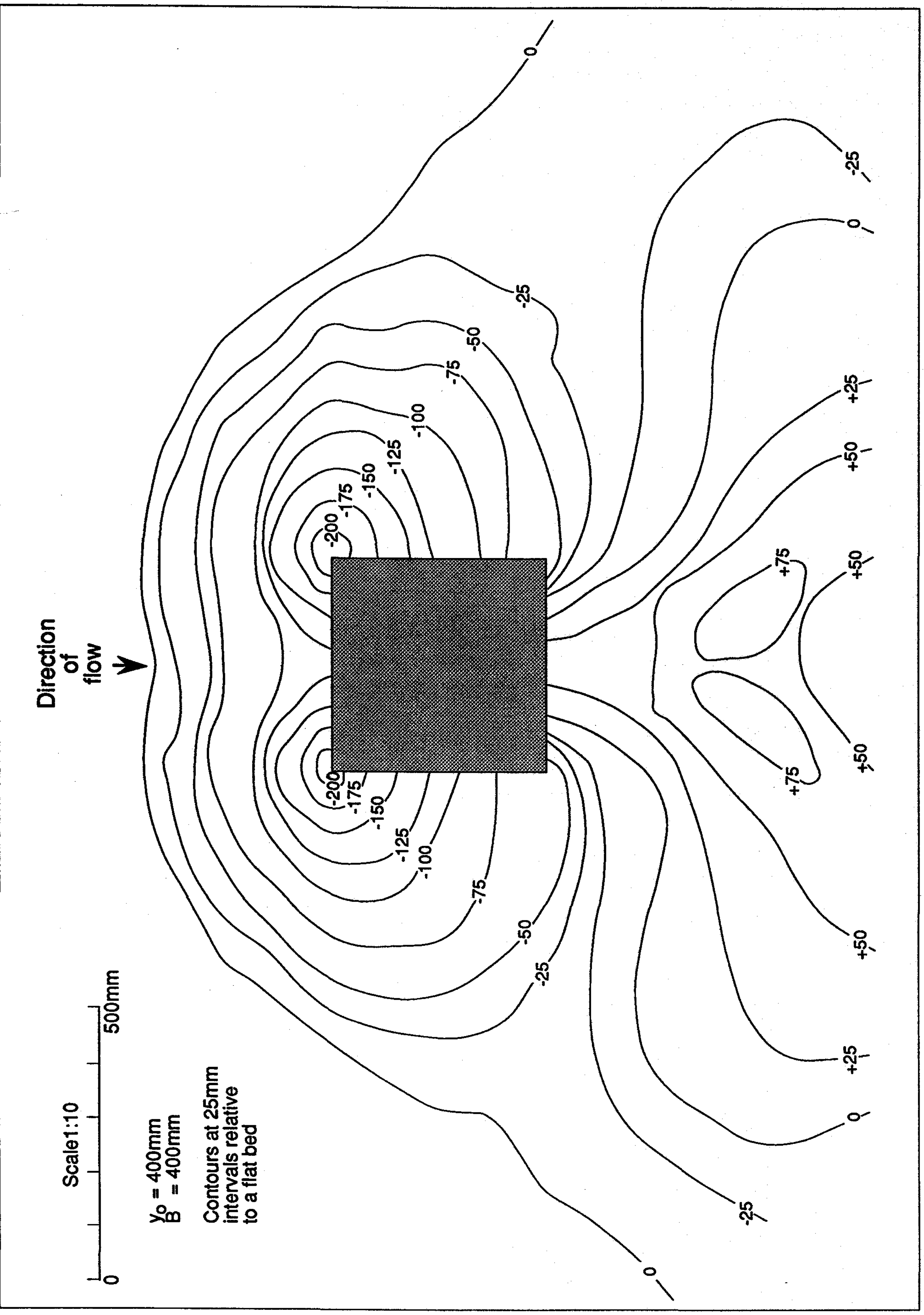

Fig 6 Scour pattern for Test S6

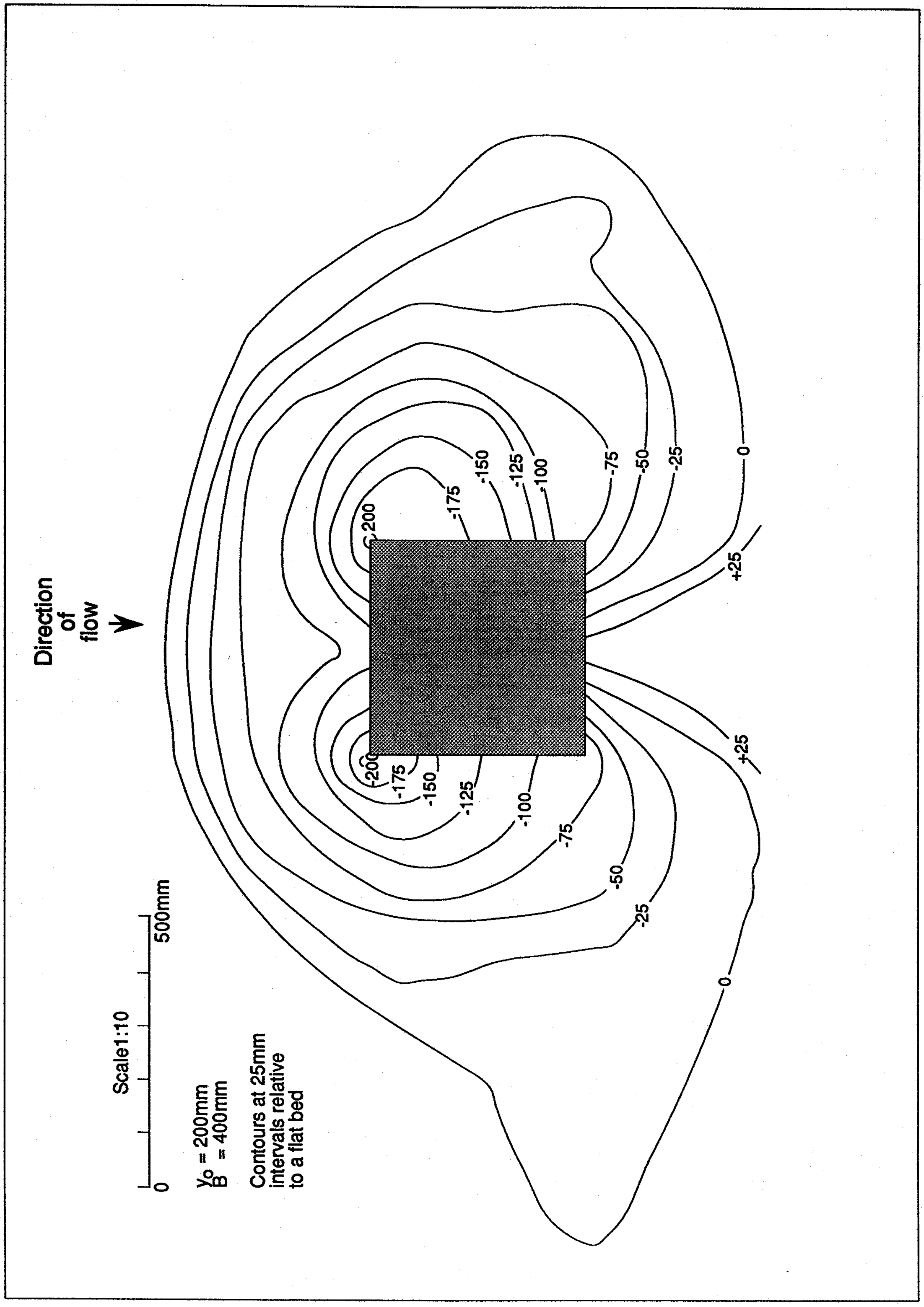

Fig 7 Scour pattern for Test S7

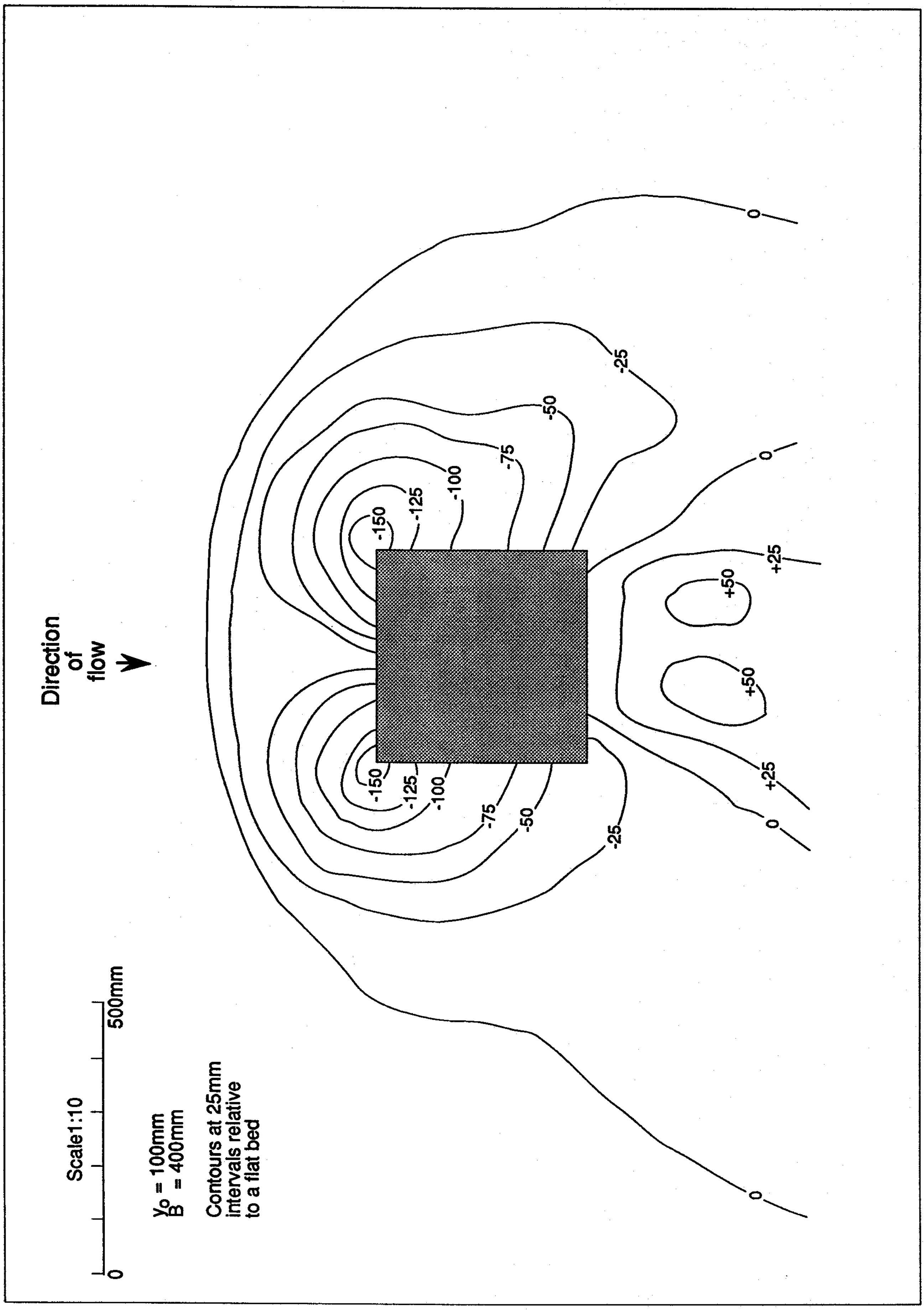

Fig 8 Scour pattern for Test S8

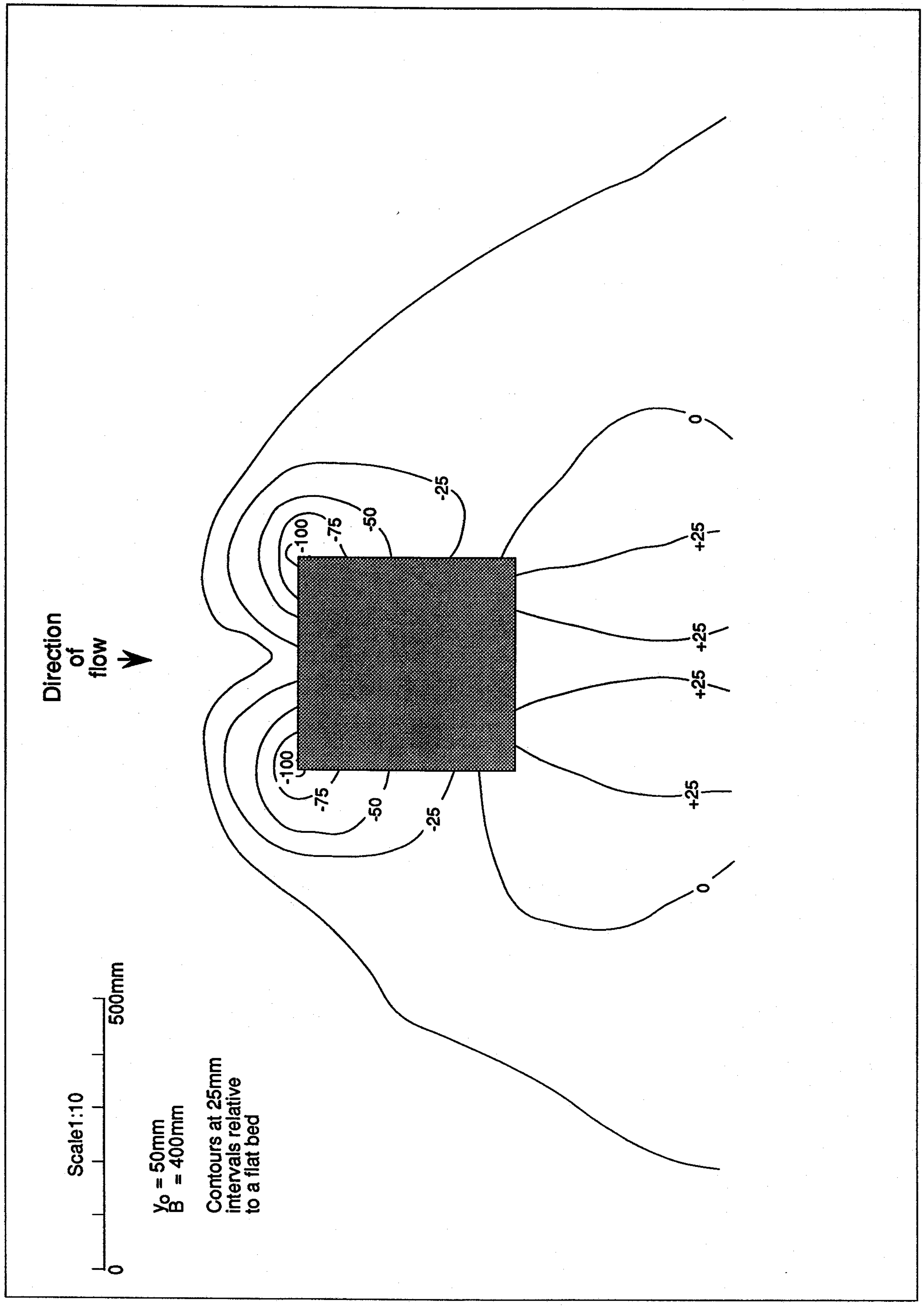

Fig 9 Scour pattern for Test S9

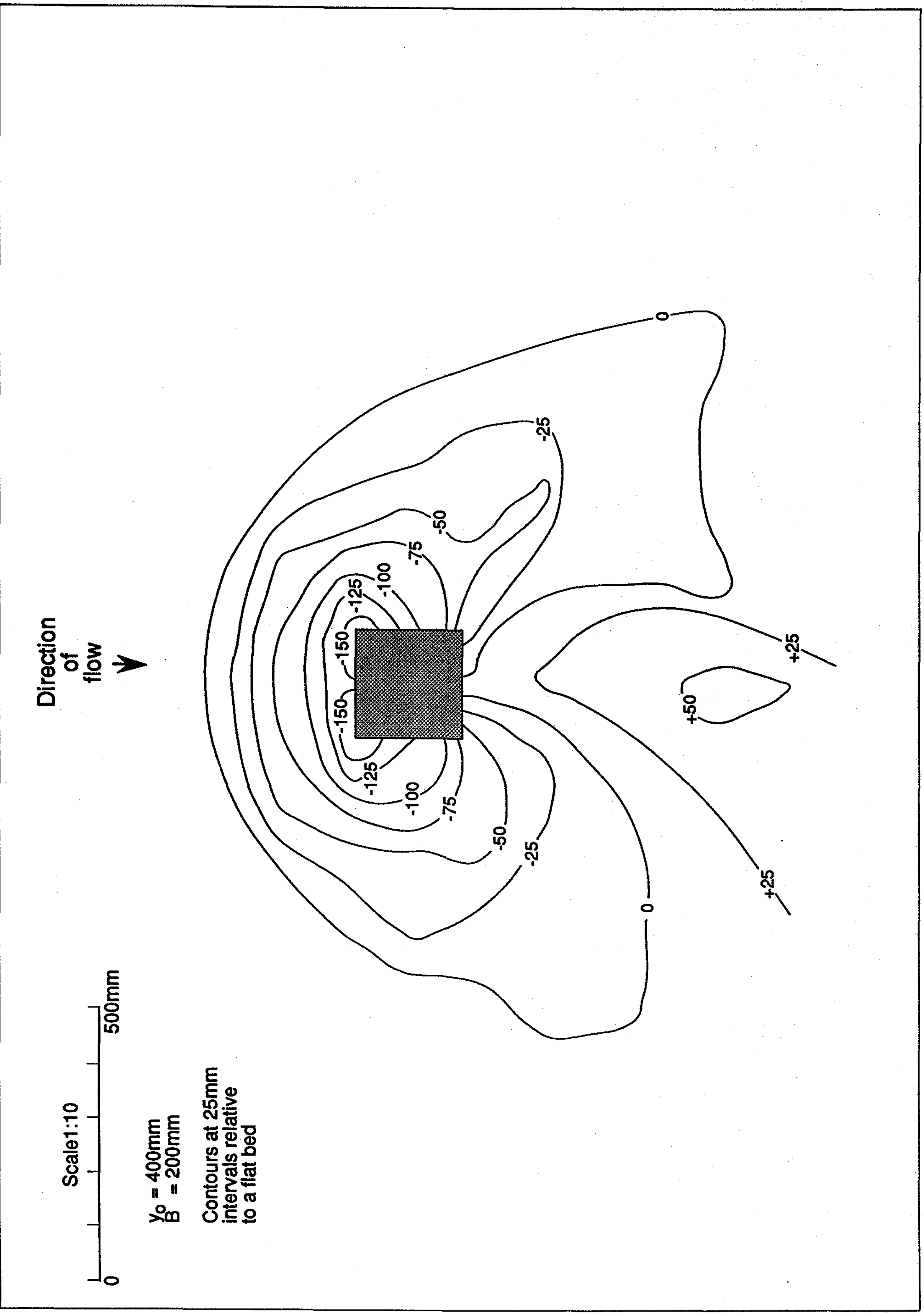

Fig 10 Scour pattern for Test S10

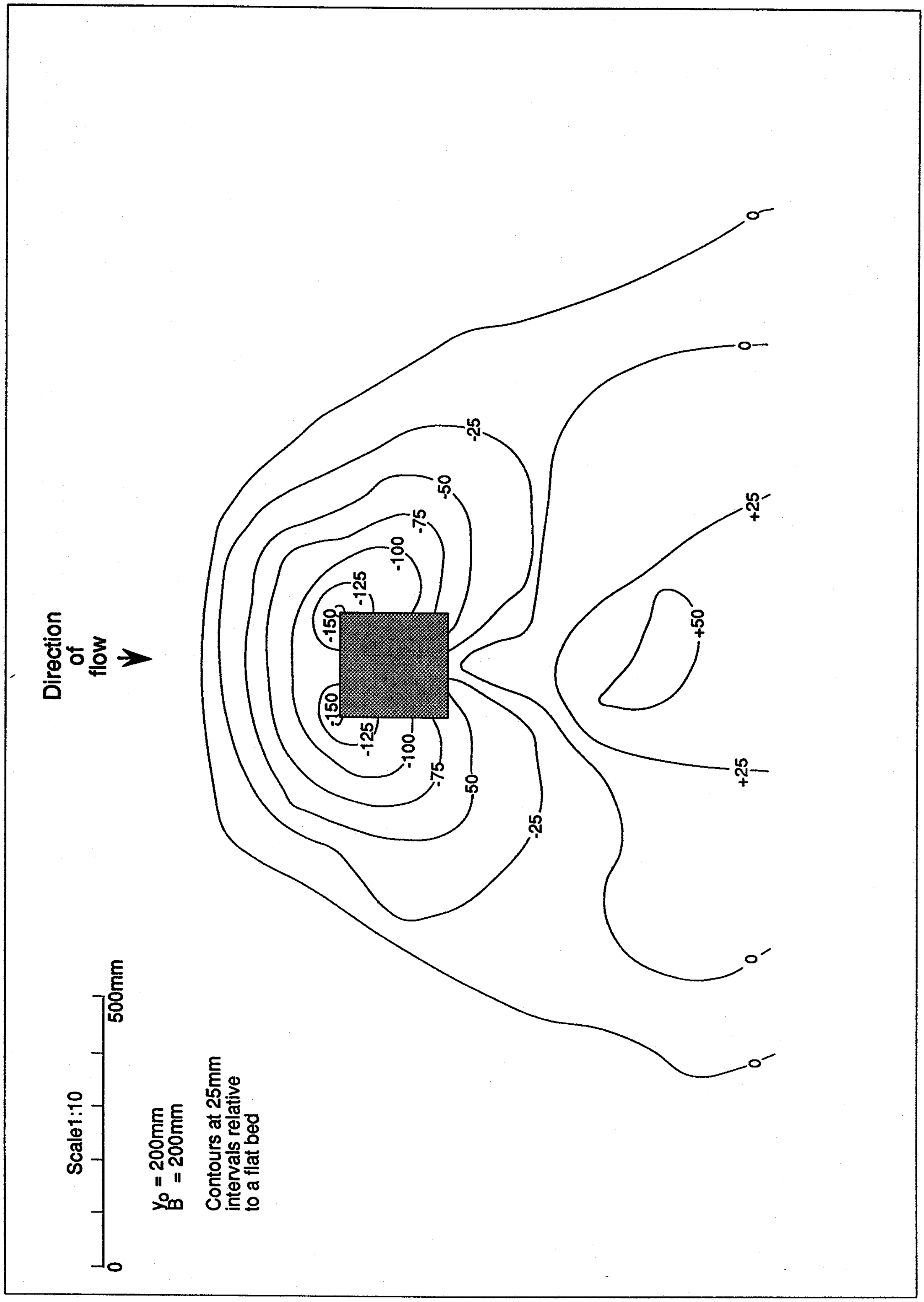

Fig 11 Scour pattern for Test S11

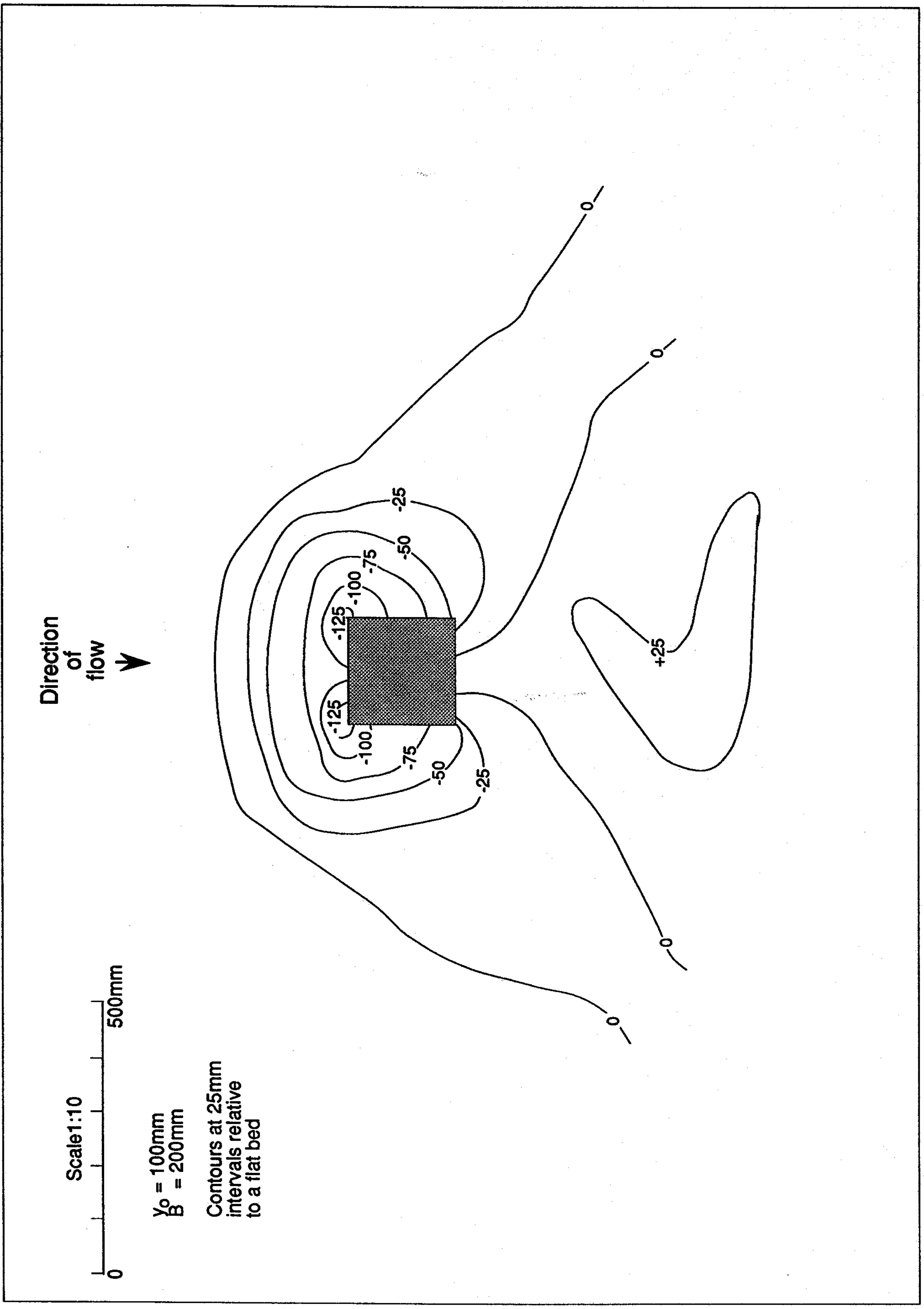

Fig 12 Scour pattern for Test S12

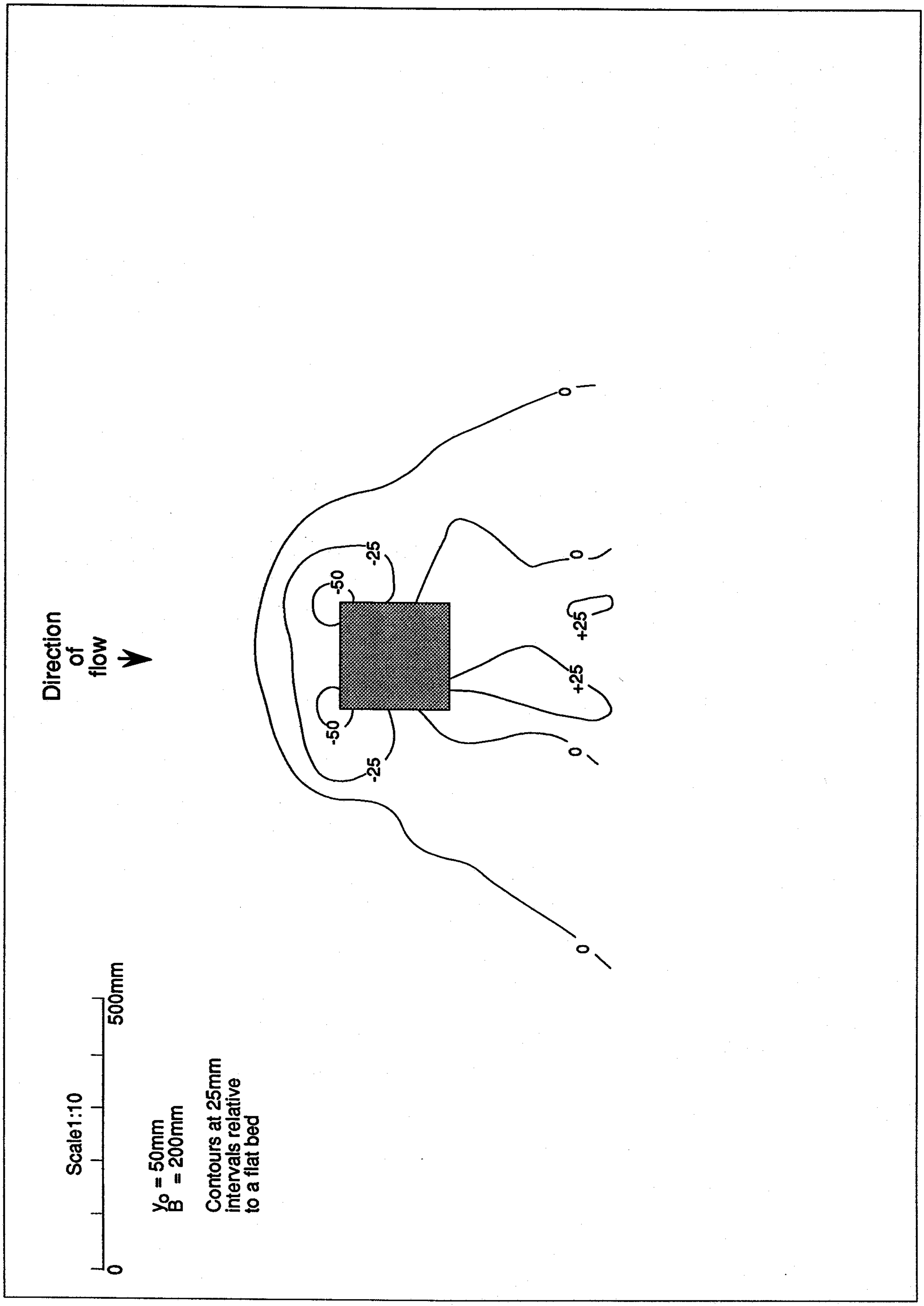

Fig 13 Scour pattern for Test S13

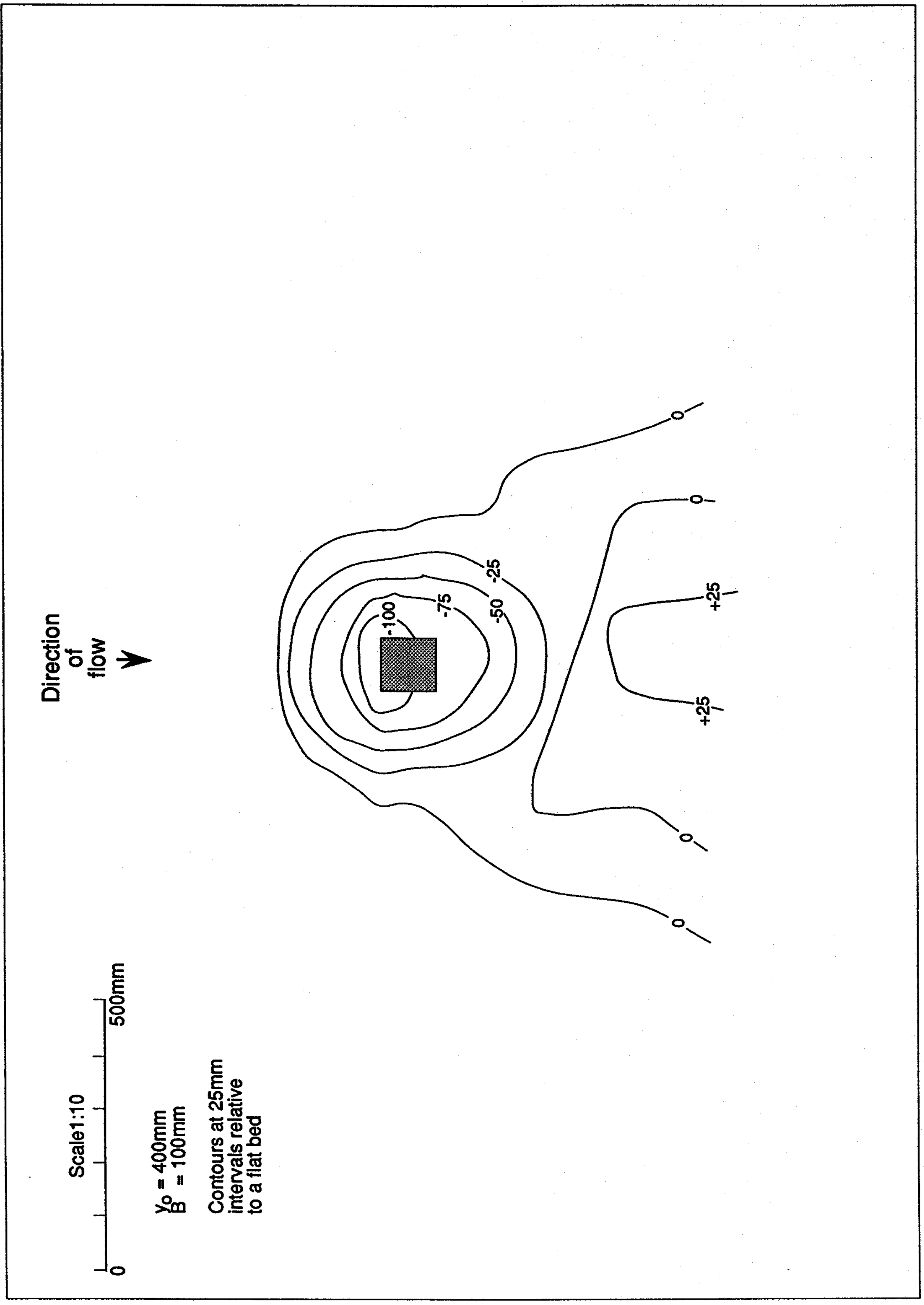

Fig 14 Scour pattern for Test S14

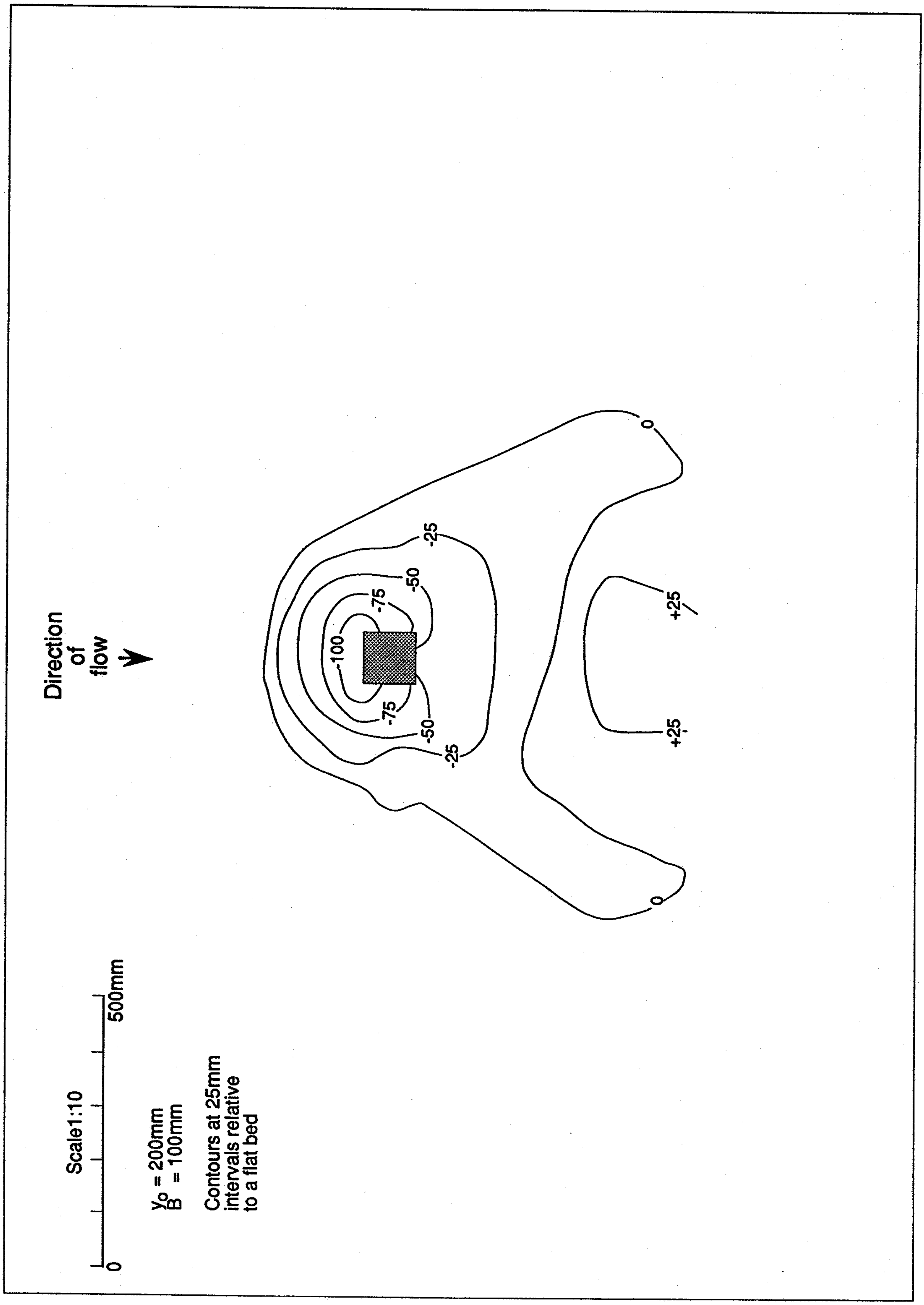

Fig 15 Scour pattern for Test S15

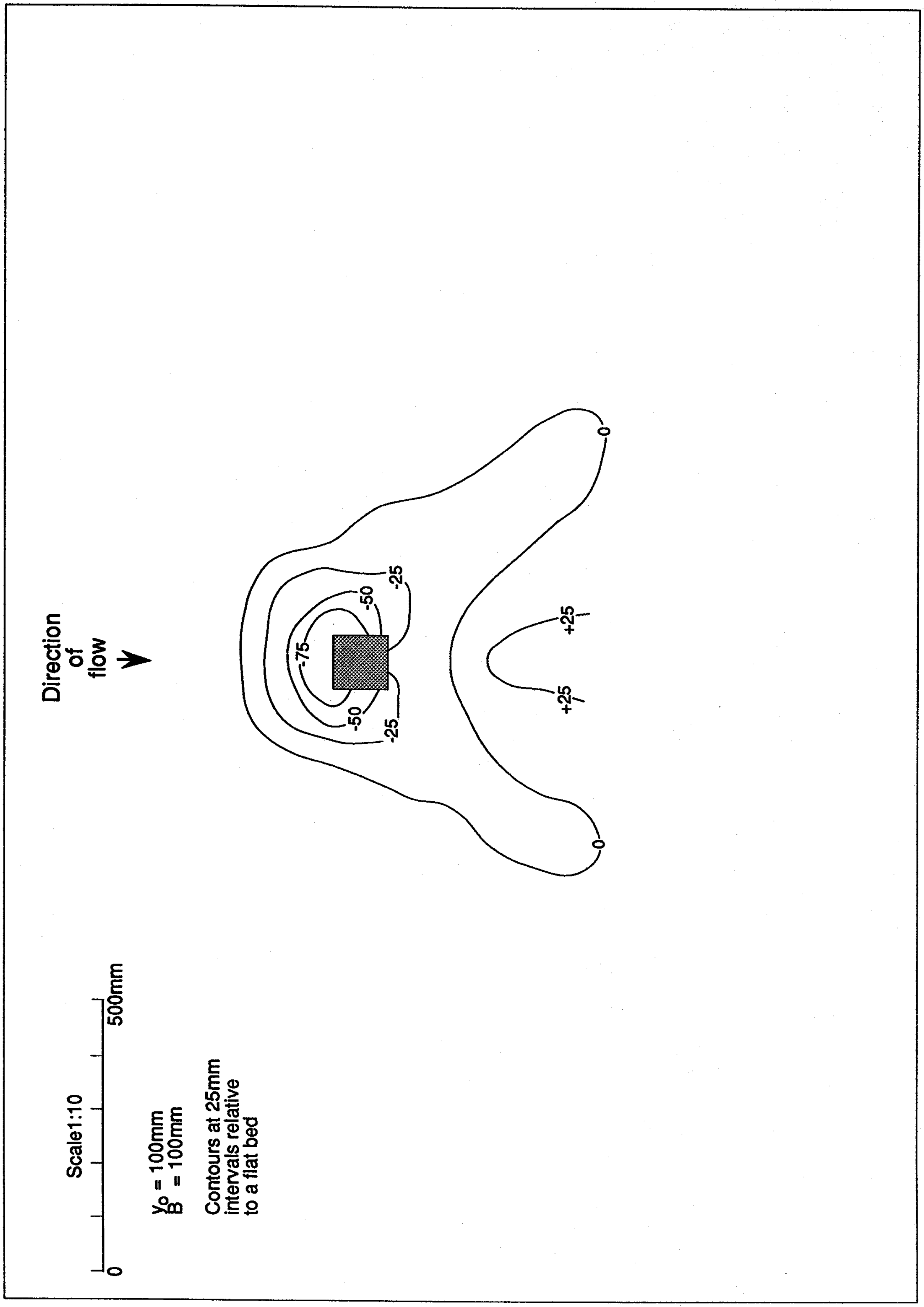

Fig 16 Scour pattern for Test S16

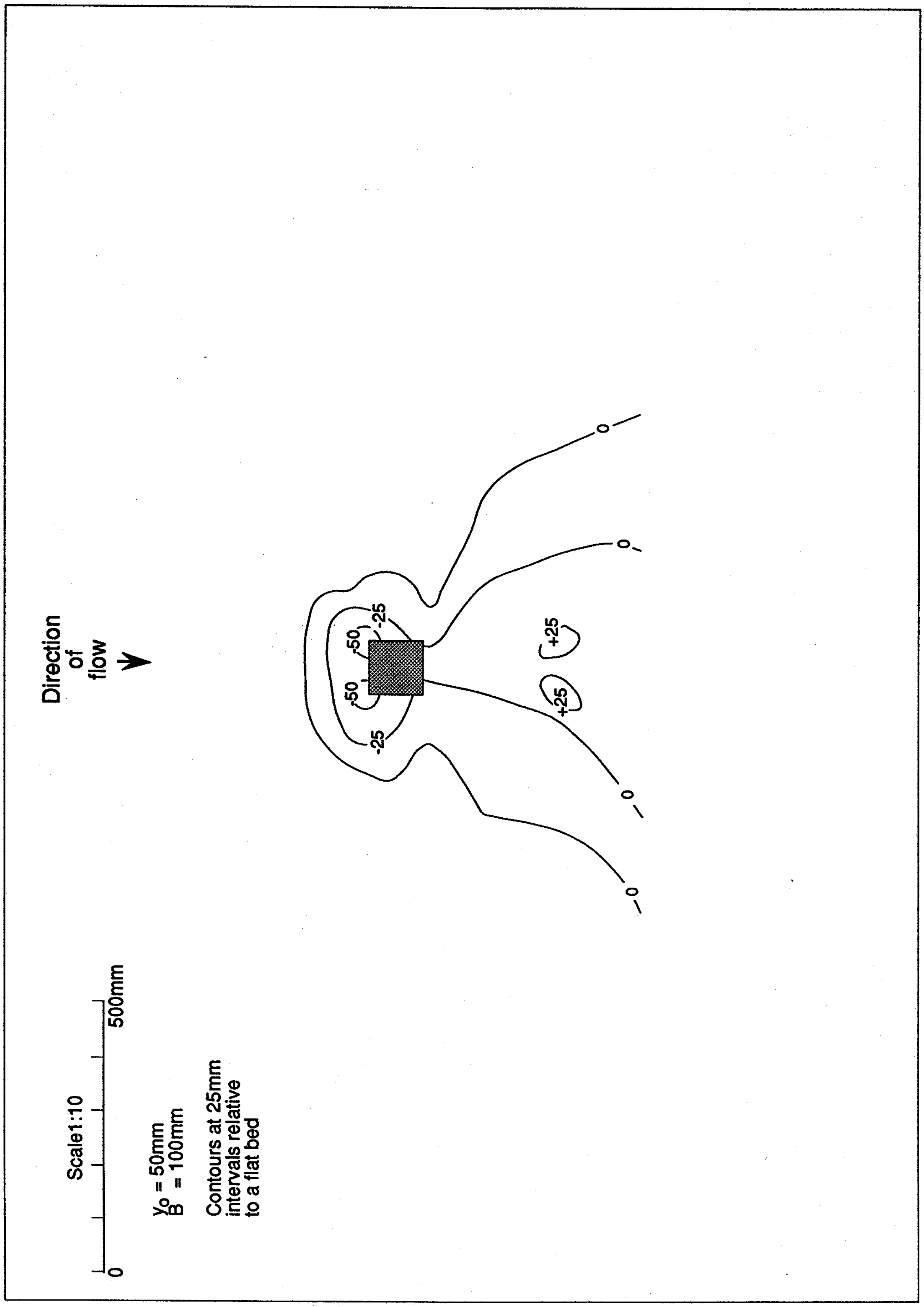

Fig 17 Scour pattern for Test S17

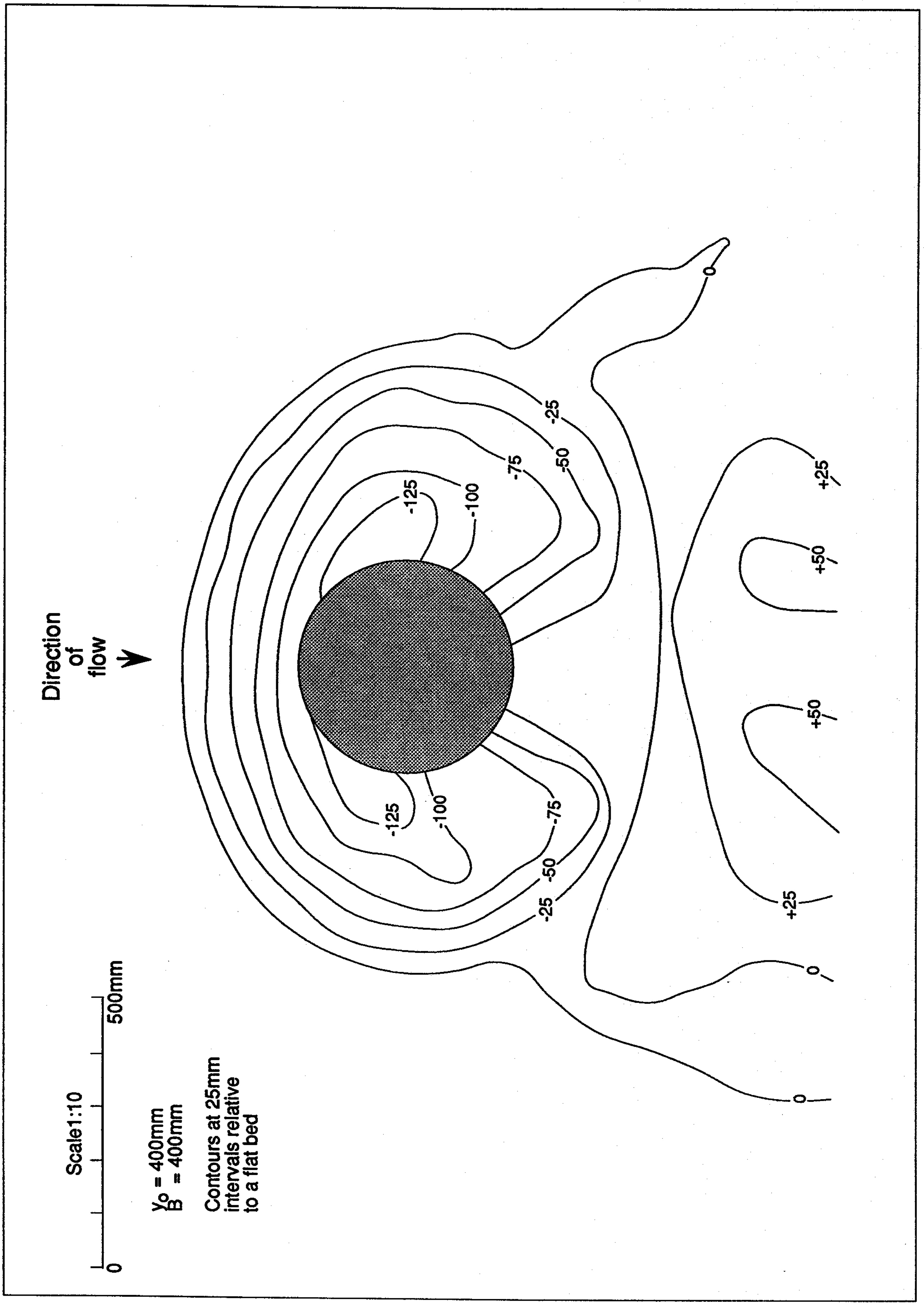

Fig 18 Scour pattern for Test C5

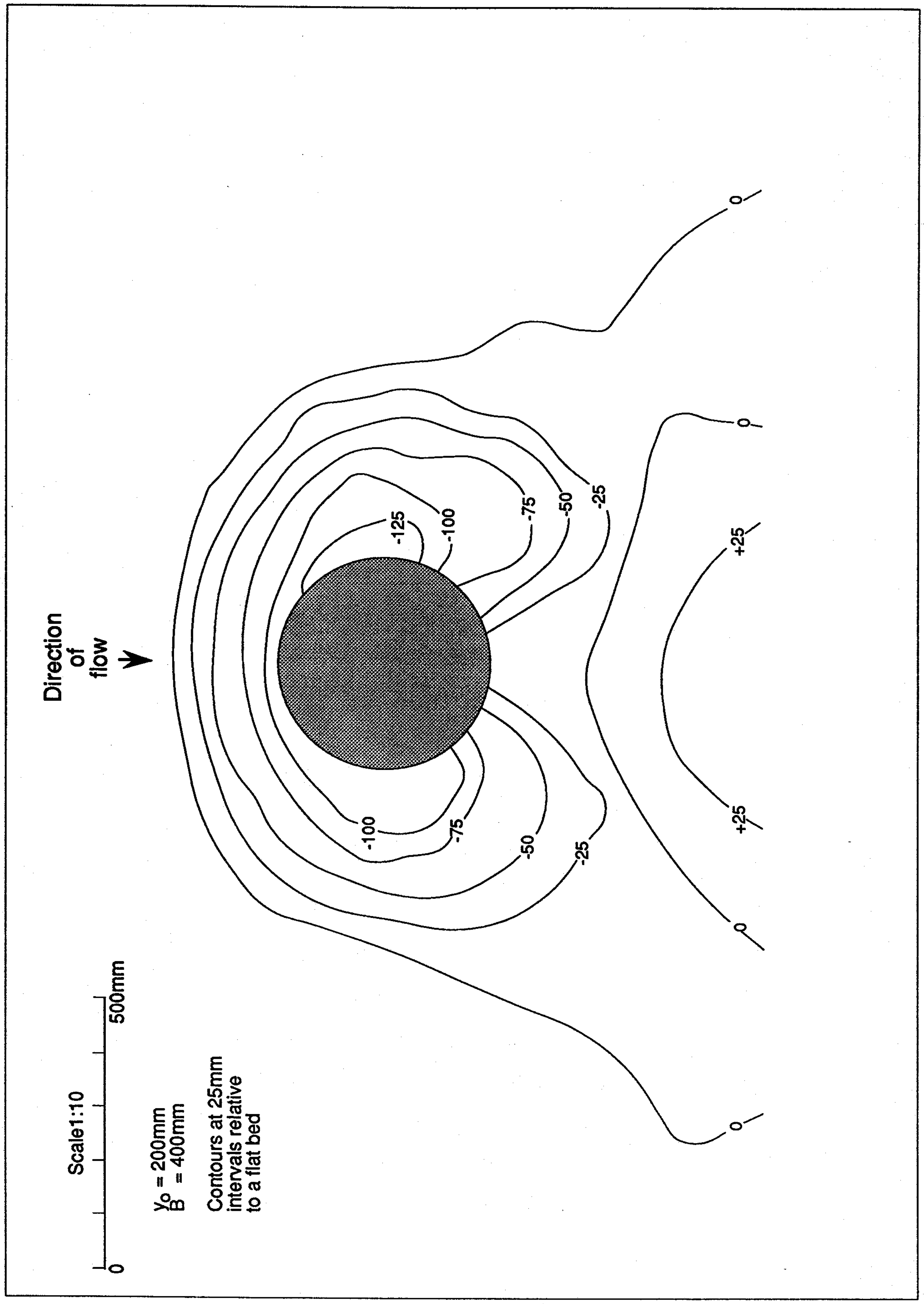

Fig 19 Scour pattern for Test C6

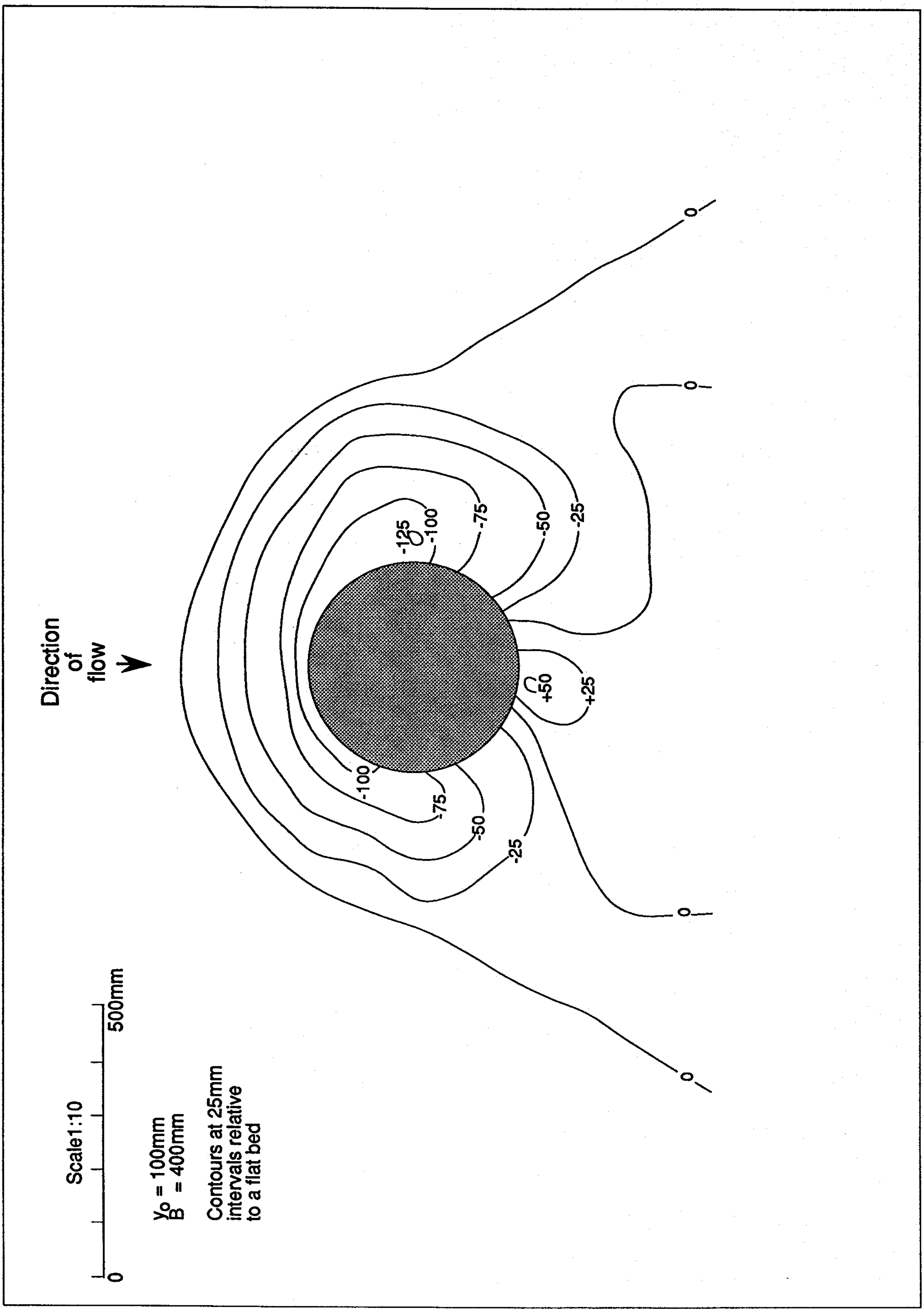

Fig 20 Scour pattern for Test C7

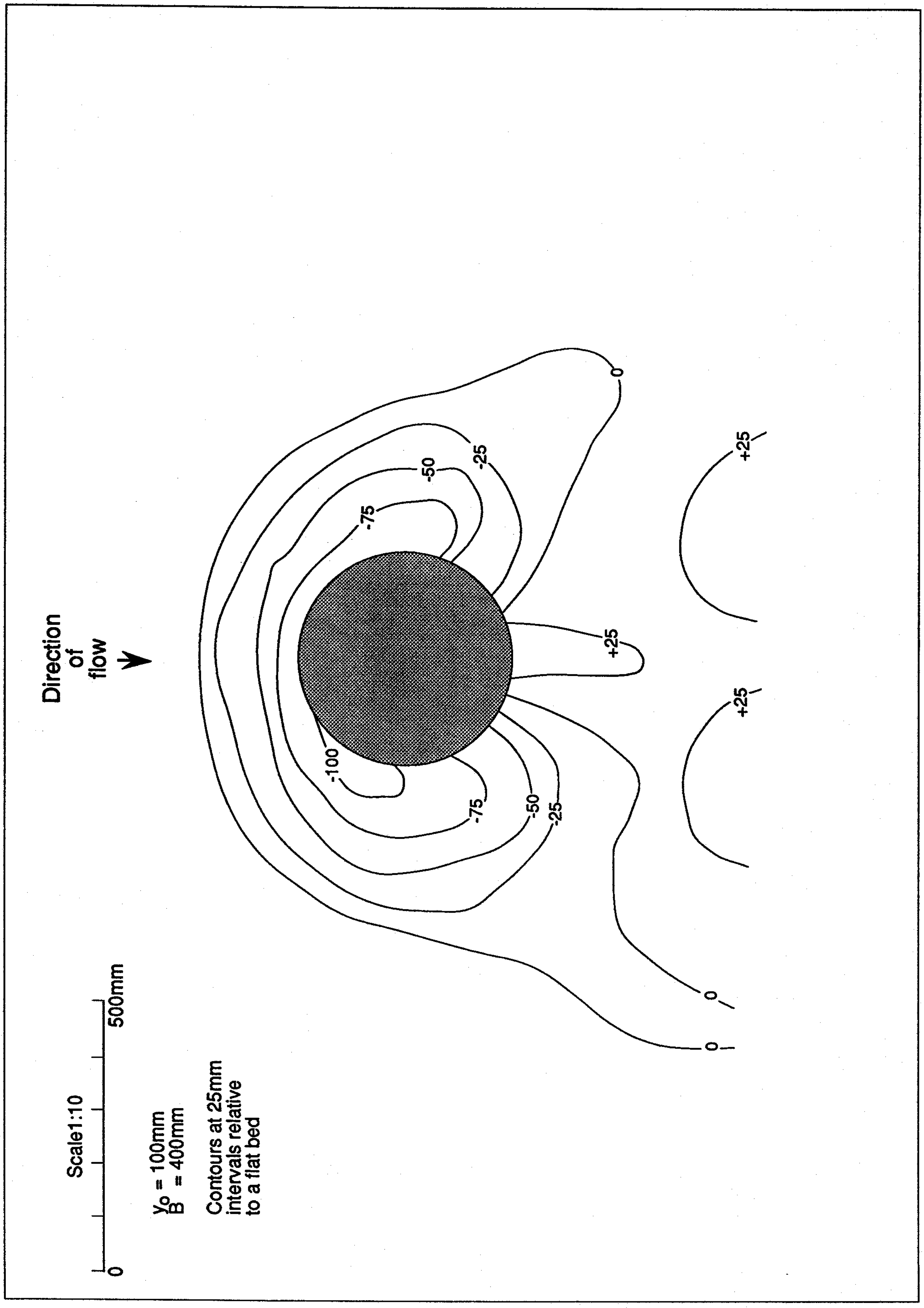

Fig 21 Scour pattern for Test C7R

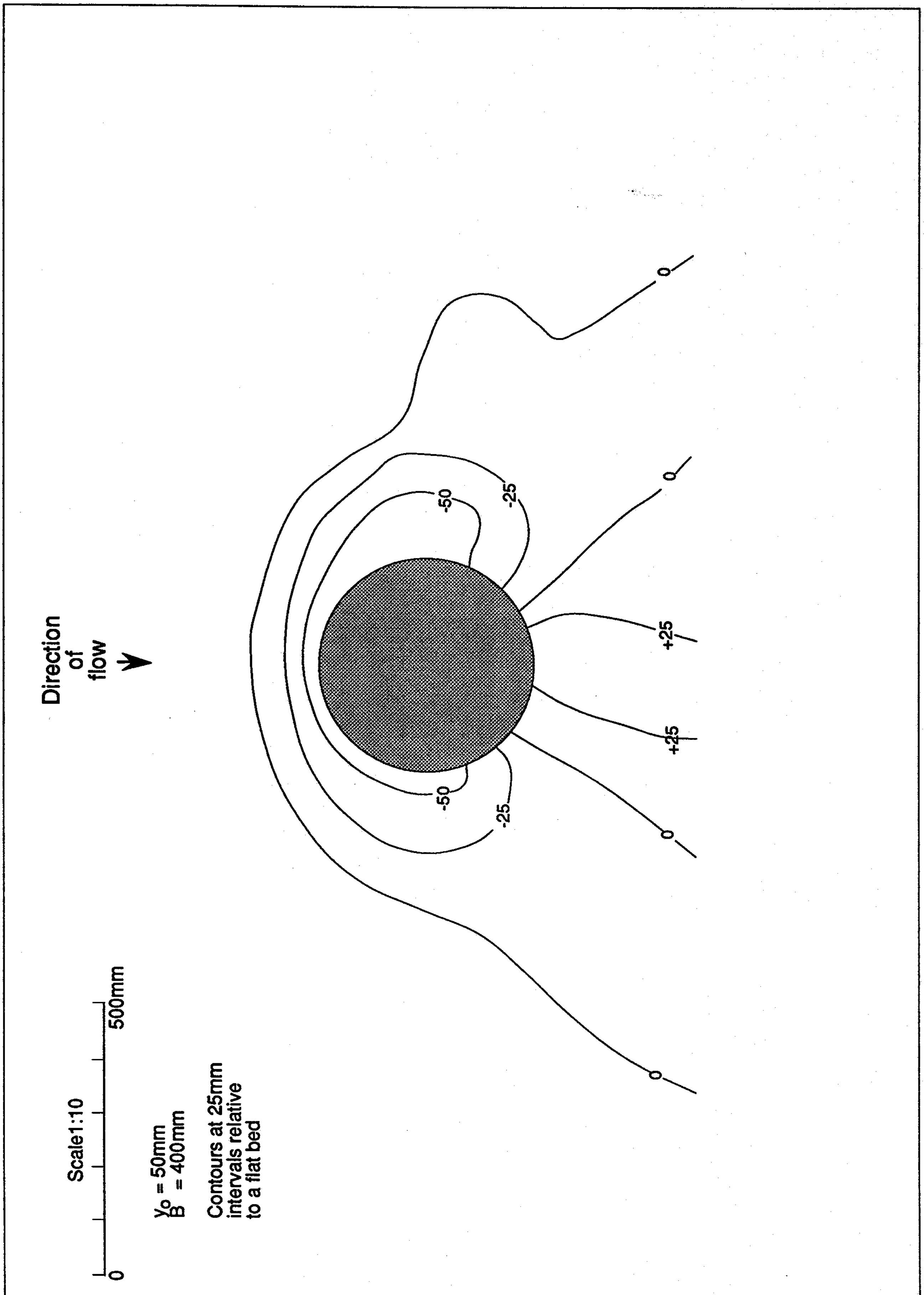

Fig 22 Scour pattern for Test C8

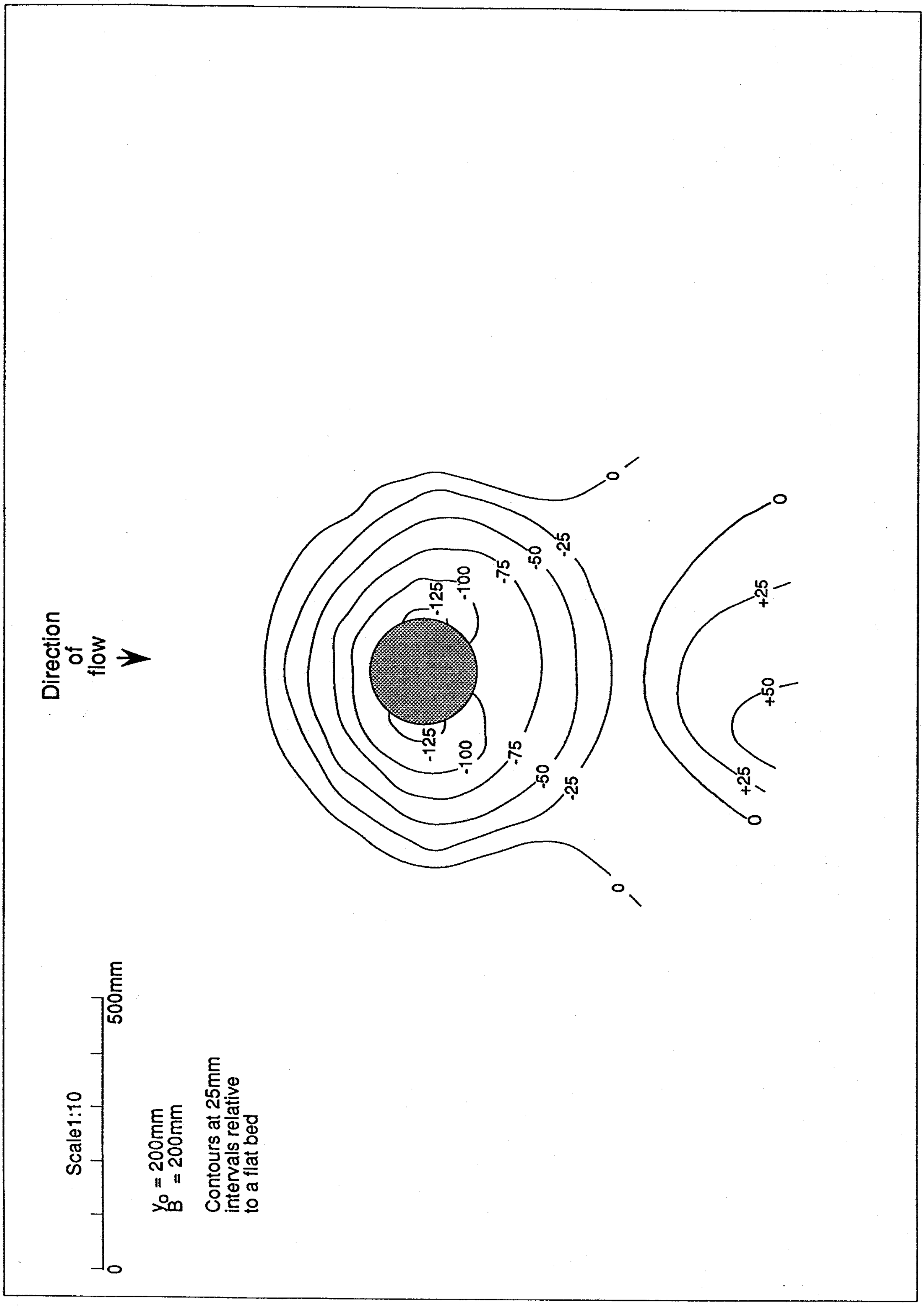

Fig 23 Scour pattern for Test C9

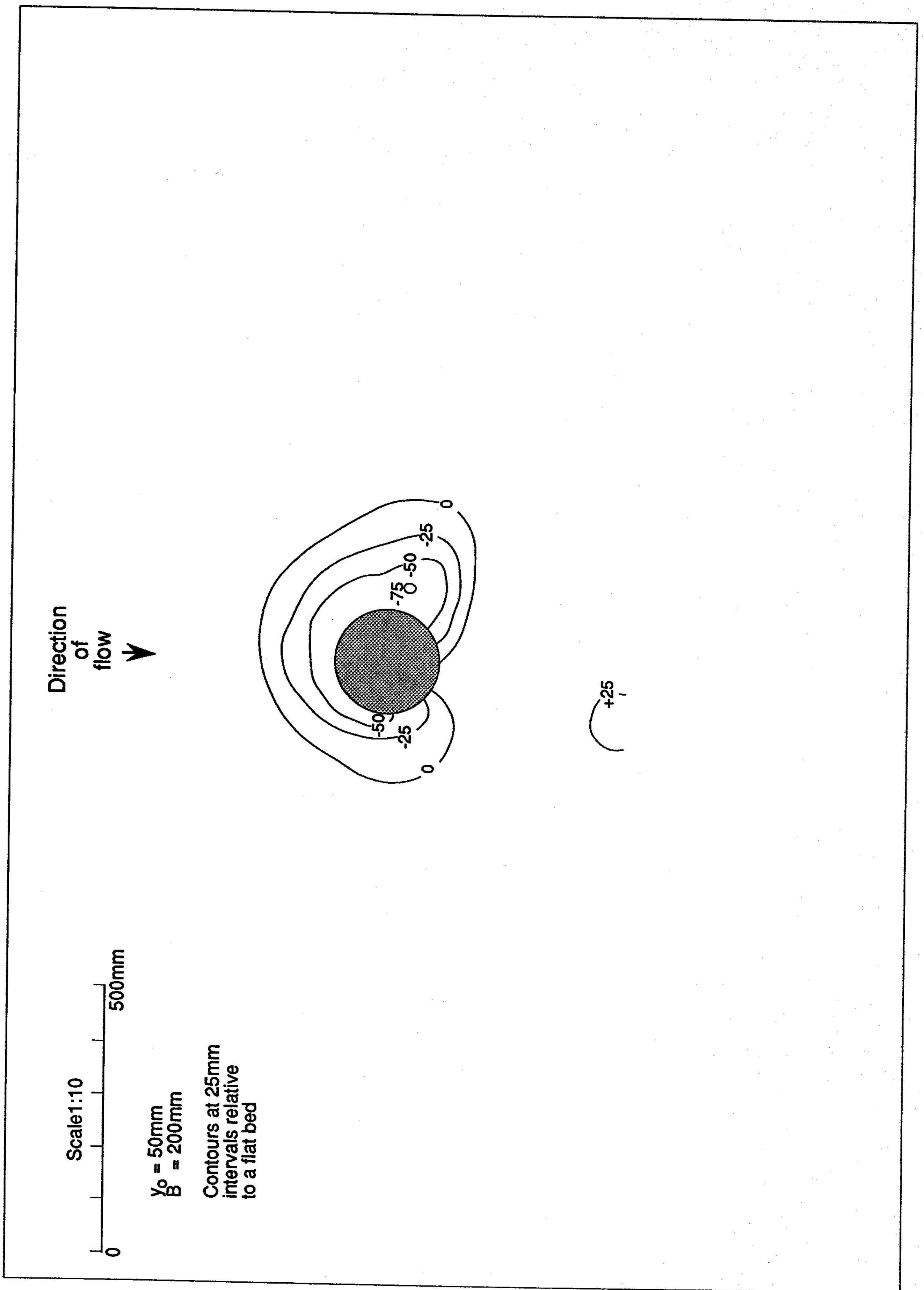

Fig 24 Scour pattern for Test C10

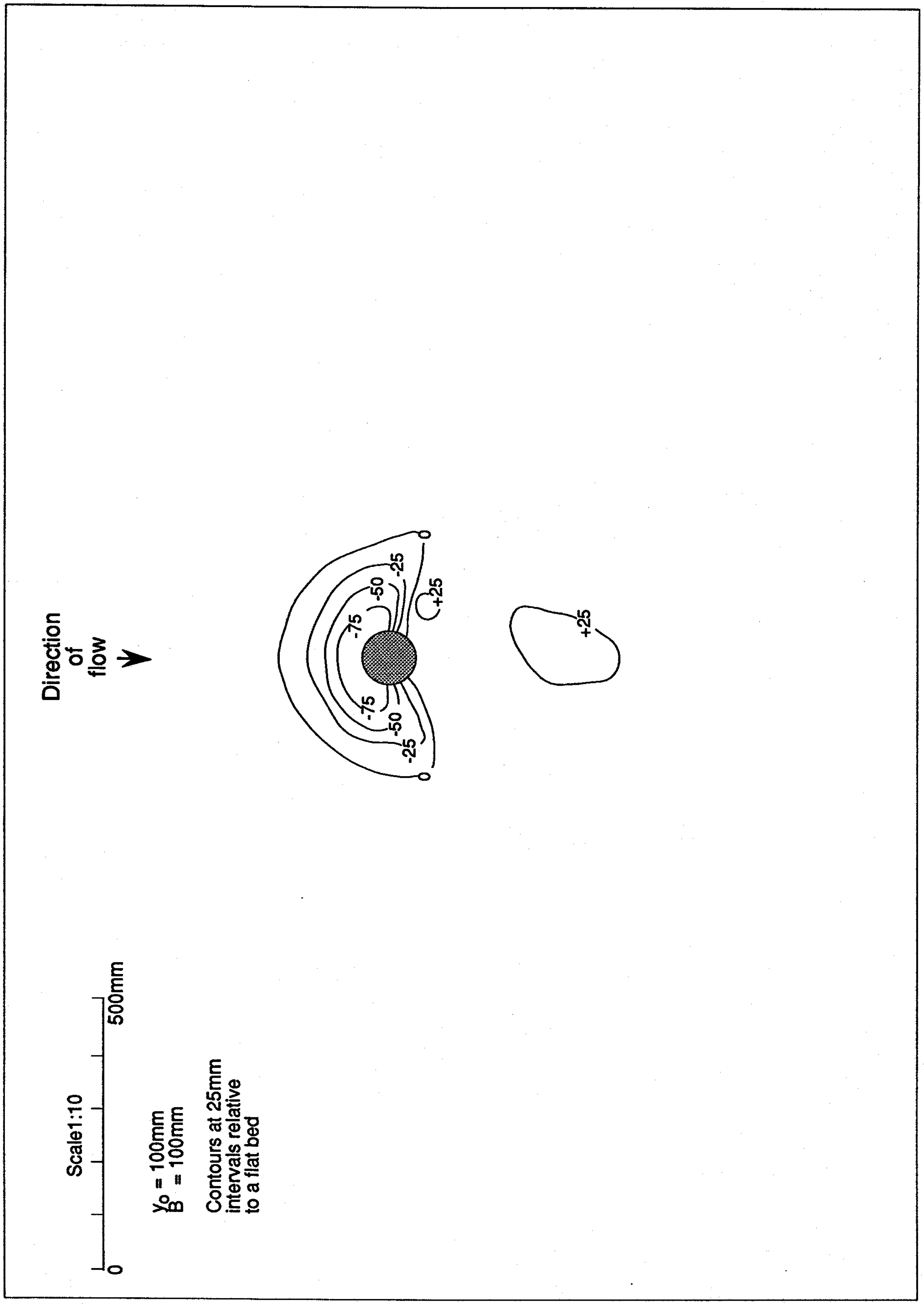

Fig 25 Scour pattern for Test C11

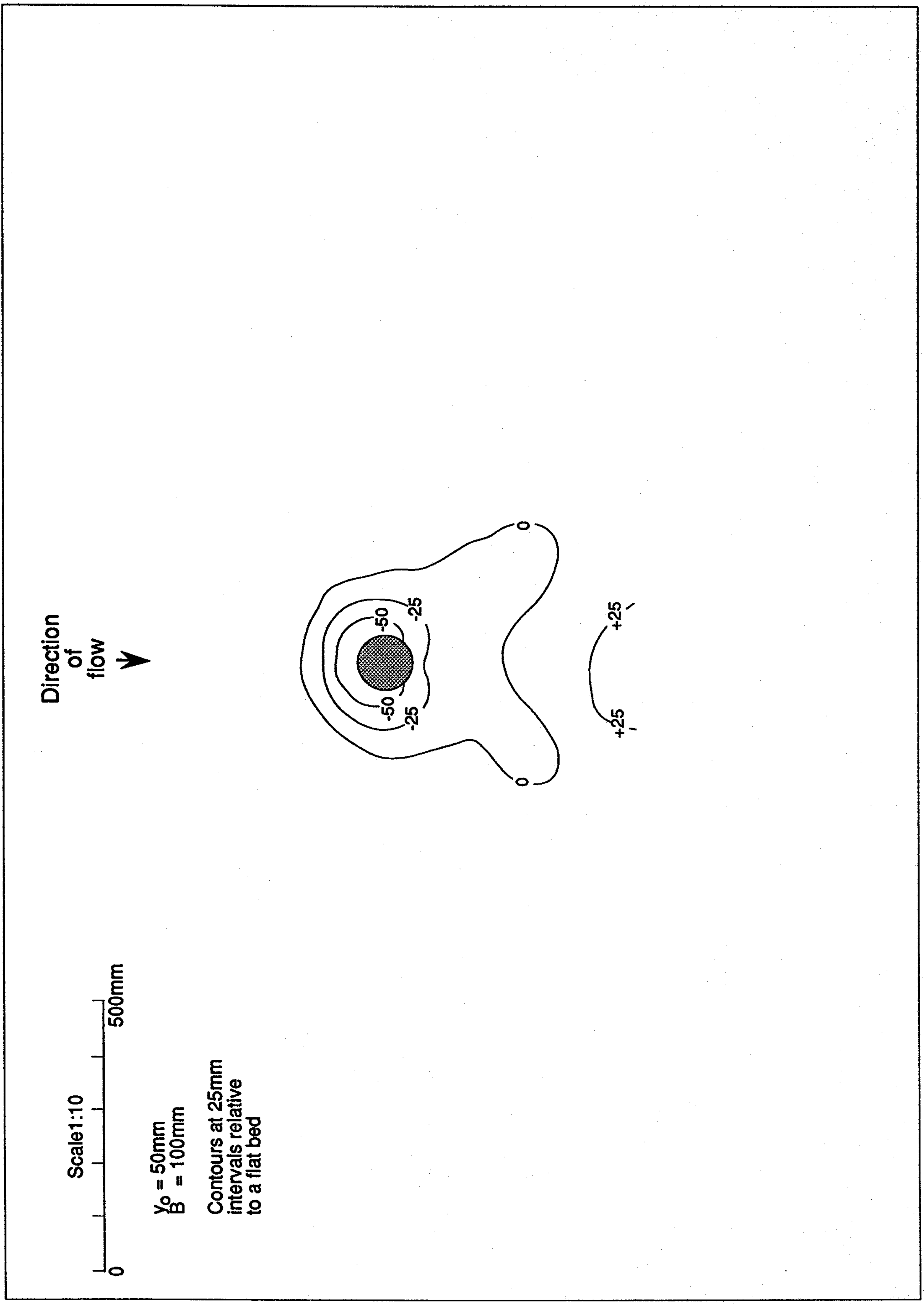

Fig 26 Scour pattern for Test C12

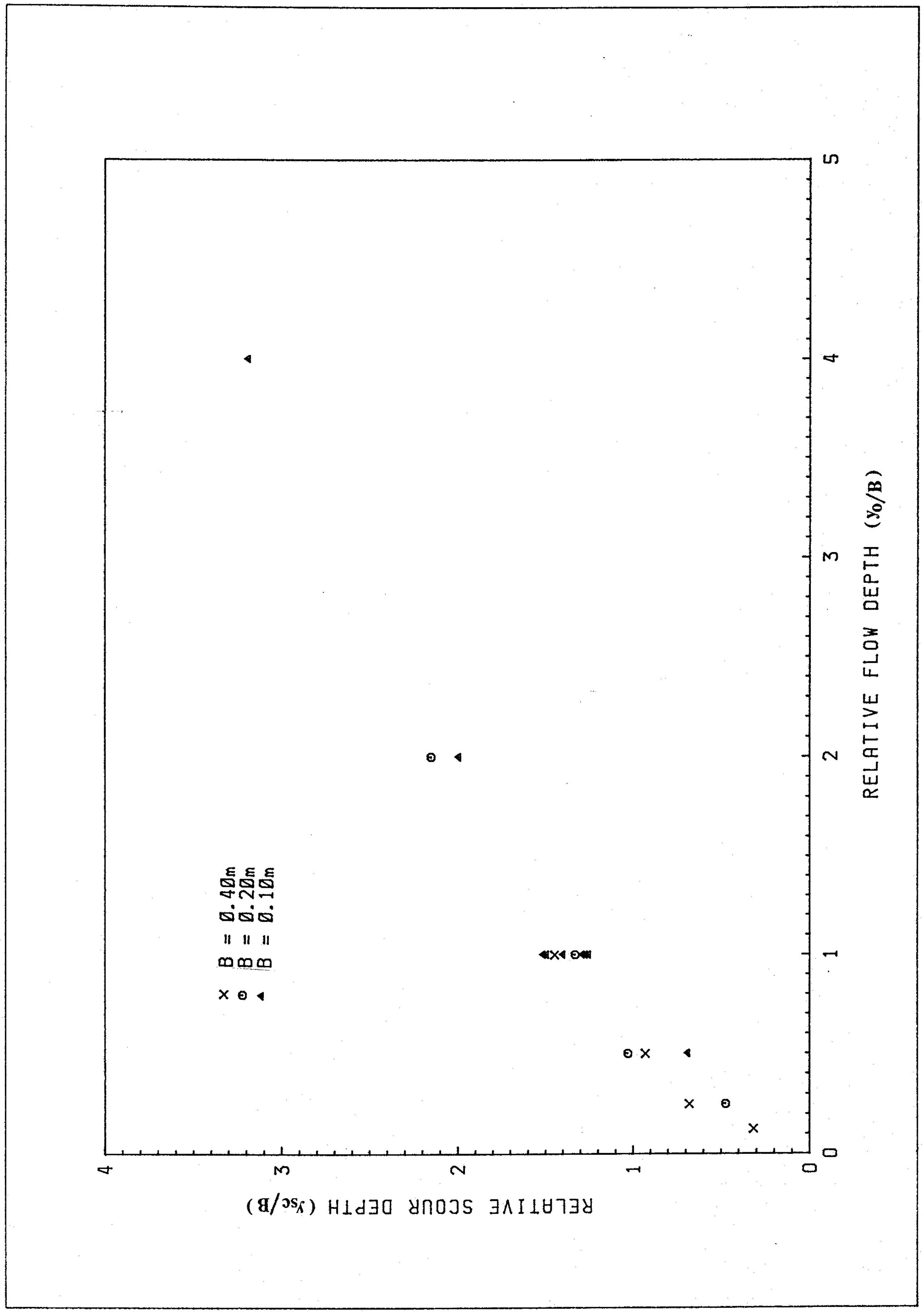

FIG 27a VARIATION OF RELATIVE SCOUR DEPTH WITH RELATIVE FLOW DEPTH - SQUARE PIERS

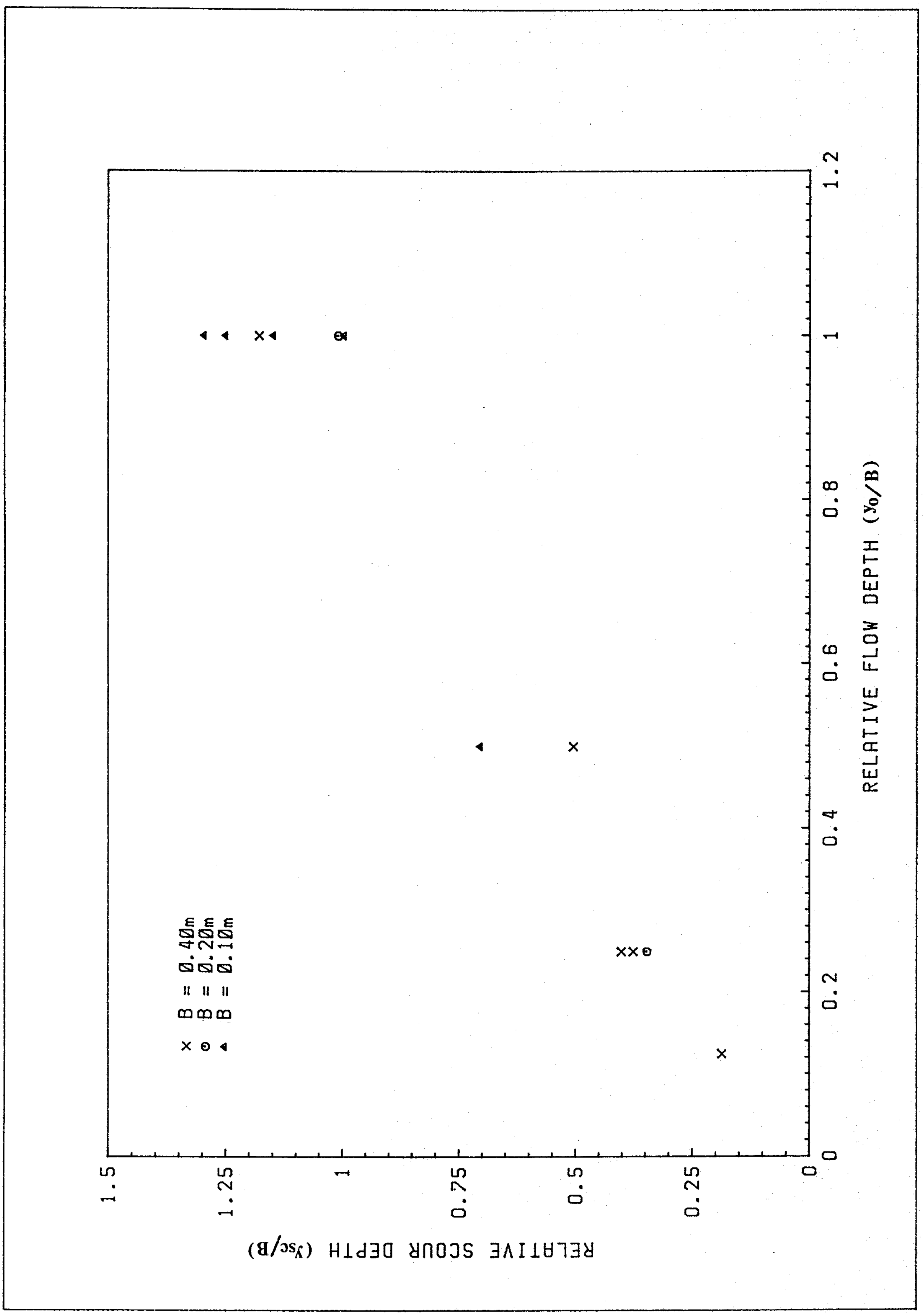

FIG 27b VARIATION OF RELATIVE SCOUR DEPTH WITH RELATIVE FLOW DEPTH - CIRCULAR PIERS

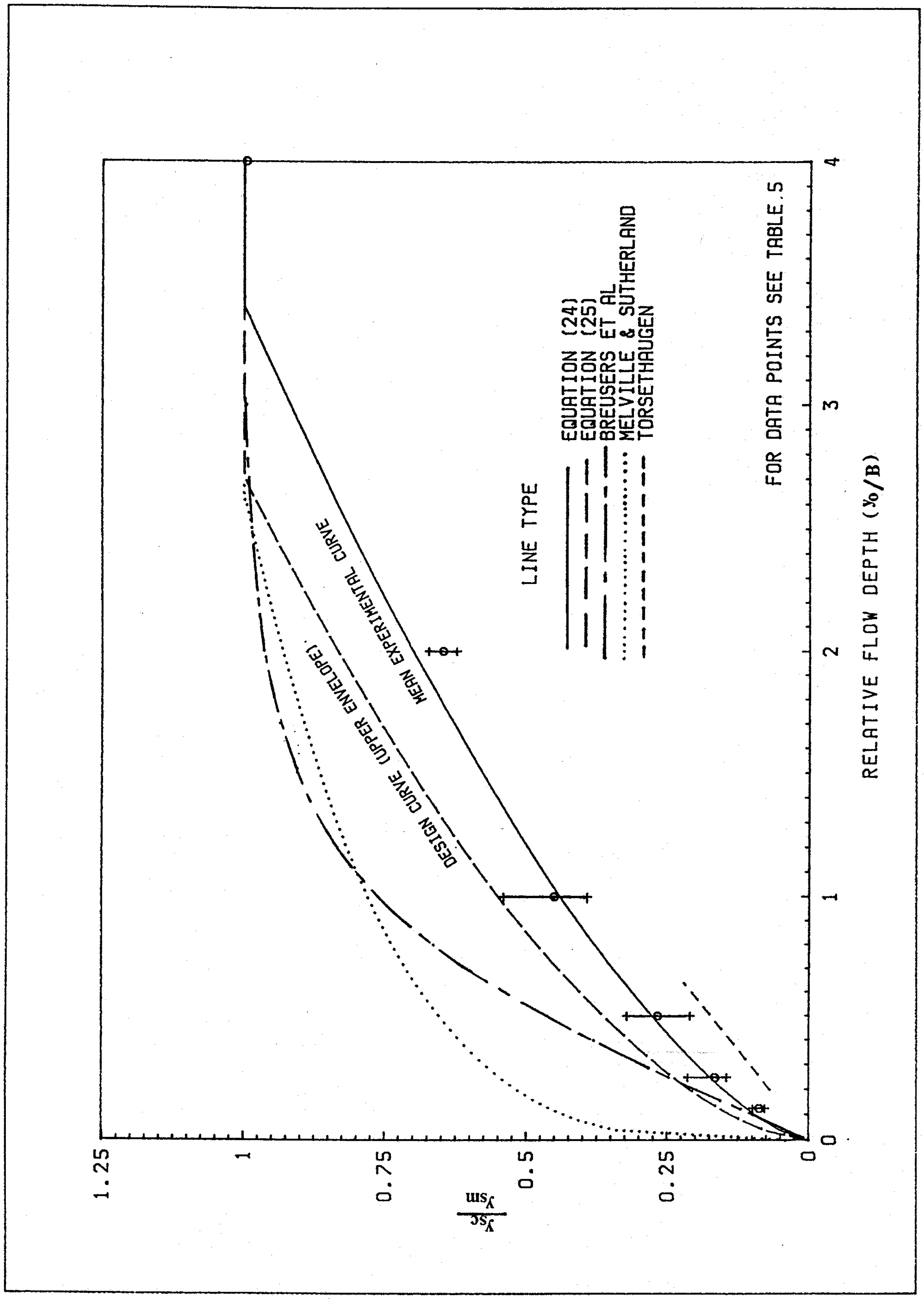

FIG 28 FUNCTION FOR EFFECT OF RELATIVE FLOW DEPTH